5

Unsteady axisymmetric and related flows

5.1 Pipe and cylinder flows

In the first part of this chapter we consider the unsteady flow within circular pipes either driven by a pressure gradient that may have both a steady and time-dependent part, or steady, with unsteadiness of the flow introduced by an unsteady motion of the pipe itself. By cylinder flows we imply the motion external to a pipe, induced by motion of the pipe itself. With the velocity vector $\mathbf{v} = \mathbf{v}(r, t)$ the governing equations are as set out in chapter 3 with the components of $\partial\mathbf{v}/\partial t$ added to equations (3.2) to (3.4) as appropriate.

5.1.1 Impulsive pipe flow

Szymański (1932) considered situations for which the fluid is at rest for $t < 0$, so that with $p = -P(t)z$ we have $P(t) \equiv 0$ for $t < 0$, and for $t > 0$ the flow is unidirectional with $v_z(r, t)$ satisfying

$$\frac{\partial v_z}{\partial t} = \frac{P}{\rho} + \nu\left(\frac{\partial^2 v_z}{\partial r^2} + \frac{1}{r}\frac{\partial v_z}{\partial r}\right), \tag{5.1}$$

with

$$v_z(r, 0) = 0, \quad 0 \le r \le a; \quad v_z(a, t) = 0, \quad \text{all} \quad t. \tag{5.2}$$

For the particular case $P =$ constant for $t > 0$, the flow approaches Poiseuille flow as $t \to \infty$ and Szymański writes

$$v_z = \frac{P}{4\mu}\left(a^2 - r^2\right) + \bar{v}_z(r, t), \tag{5.3}$$

so that with $\bar{v}_z(r, t) = \bar{V}(r)\,\mathrm{e}^{-\nu\lambda^2 t/a^2}$, $\bar{V}(r)$ satisfies

$$r\bar{V}'' + \bar{V}' + (\lambda^2 r/a^2)\bar{V} = 0,$$

with solution that is bounded at $r = 0$ and vanishes at $r = a$, $\bar{V}(r) = J_0(\lambda_n r/a)$ where λ_n is a solution of $J_0(\lambda_n) = 0$. The complete solution of (5.3) may then be written as

$$v_z = \frac{P}{4\mu}\left(a^2 - r^2\right) + \sum_{n=0}^{\infty} C_n J_0(\lambda_n r/a)\, \mathrm{e}^{-\nu\lambda_n^2 t/a^2},$$

where the constants C_n are determined from the condition $v_z(r, 0) = 0$ as

$$C_n = \frac{2Pa^2}{\mu\lambda_n^3 J_0'(\lambda_n)}.$$

Szymański also considers cases for which $P(t)$ is a periodic function of time, and $P(t) \to$ constant as $t \to \infty$; whilst Smith (1997) addresses the case for which $P(t) \propto k^2 \mathrm{e}^{-\nu k^2 t}$.

5.1.2 Periodic pipe flow

Situations for which $p = -Pz + f(t)z$ where $f(t)$ is a periodic function of time for all t have been studied by Sexl (1930), Lambossy (1952), Womersley (1955a, 1955b) and Uchida (1956). In Womersley's case the motivation for the study was physiological, in connection with the flow of blood in the larger arteries. Since $f(t)$ can be represented as a Fourier series, and since the governing equations are linear we may, without loss of generality, consider a single frequency and let

$$\frac{\partial p}{\partial z} = -P - c_1 \cos\omega t - c_2 \sin\omega t = -P - c\, \mathrm{e}^{\mathrm{i}\omega t}, \quad c = c_1 - \mathrm{i}c_2, \tag{5.4}$$

where, as in chapter 4, the real part of any complex quantity is to be understood. We may now write

$$v_z(r, t) = \frac{P}{4\mu}\left(a^2 - r^2\right) + \tilde{v}_z(r, t) \tag{5.5}$$

where, from (5.1) and (5.4), $\tilde{v}(r, t)$ satisfies

$$\frac{\partial \tilde{v}_z}{\partial t} = \frac{c}{\rho}\mathrm{e}^{\mathrm{i}\omega t} + \nu\left(\frac{\partial^2 \tilde{v}_z}{\partial r^2} + \frac{1}{r}\frac{\partial \tilde{v}_z}{\partial r}\right) \tag{5.6}$$

and, seeking a separable solution with $\tilde{v}_z = c\tilde{V}(r)\, \mathrm{e}^{\mathrm{i}\omega t}/\rho$ we have

$$r\tilde{V}'' + \tilde{V}' + \mathrm{i}^3 k^2 r\tilde{V} = -\frac{r}{\nu} \quad \text{where} \quad k^2 = \frac{\omega}{\nu}. \tag{5.7}$$

The solution of (5.7) for $\tilde{V}$ which is bounded at $r = 0$, and satisfies the no-slip condition at $r = a$, is

$$\tilde{V} = \left(\frac{J_0(\mathrm{i}^{3/2}kr)}{J_0(\mathrm{i}^{3/2}ka)} - 1\right)\frac{\mathrm{i}}{\omega},$$

so that if we introduce Kelvin's functions ber and bei with

$$J_0(\mathrm{i}^{3/2}x) = \mathrm{ber}(x) + \mathrm{ibei}(x),$$

we have, finally,

$$\tilde{v}_z = \left\{\frac{c_1F_2 + c_2(F_1 - 1)}{\rho\omega}\right\}\cos\omega t + \left\{\frac{c_2F_2 + c_1(F_1 - 1)}{\rho\omega}\right\}\sin\omega t,$$

where

$$F_1(kr) = \frac{\mathrm{ber}(kr)\mathrm{ber}(ka) + \mathrm{bei}(kr)\mathrm{bei}(ka)}{\mathrm{ber}^2(ka) + \mathrm{bei}^2(ka)},$$

$$F_2(kr) = \frac{\mathrm{ber}(kr)\mathrm{bei}(ka) - \mathrm{bei}(kr)\mathrm{ber}(ka)}{\mathrm{ber}^2(ka) + \mathrm{bei}^2(ka)}.$$

The instantaneous volume flux across any section is given by

$$\begin{aligned} Q &= \int_0^a 2\pi v_z r\,\mathrm{d}r \\ &= \frac{P\pi a^4}{8\mu} + \frac{\pi a^4}{\mu}\left\{2c_1\frac{F_1'(ka)}{(ka)^3} - \frac{c_2}{(ka)^2}\left(2\frac{F_2'(ka)}{ka} + 1\right)\right\}\cos\omega t \\ &\quad + \frac{\pi a^4}{\mu}\left\{2c_2\frac{F_1'(ka)}{(ka)^3} + \frac{c_1}{(ka)^2}\left(2\frac{F_2'(ka)}{ka} + 1\right)\right\}\sin\omega t, \end{aligned}$$

and in figure 5.1 we show appropriate coefficients of Q as a function of ka.

Sanyal (1956) has considered pipe flows for which the pressure gradient is either increasing or decreasing exponentially with time. The treatment of the problem closely follows that above, with ω taken to be a purely imaginary quantity.

5.1.3 Pulsed pipe flow

Lance (1956) considered the modifications to Poiseuille flow in a pipe of radius a when the pipe itself is subjected to a series of axial pulses. With v_z represented as in equation (5.5), $\tilde{v}_z$ satisfies (5.6) but with $c \equiv 0$. The boundary conditions for $\tilde{v}_z$ now require

$$\tilde{v}_z(r,t) = 0, \quad t < 0; \quad \tilde{v}_z(a,t) = \sum_{n=0}^{N} U_n\delta(t - nt_0), \quad t > 0.$$

So, for $t > 0$ the pipe wall is subjected to a series of pulses, each represented by a delta function, at intervals t_0 and of strength U_n. If $\bar{\tilde{v}}_z$ denotes the Laplace transform of $\tilde{v}_z$, then $\bar{\tilde{v}}_z$ satisfies

$$r\frac{\mathrm{d}^2\bar{\tilde{v}}_z}{\mathrm{d}r^2} + \frac{\mathrm{d}\bar{\tilde{v}}_z}{\mathrm{d}r} - \frac{rs}{\nu}\bar{\tilde{v}}_z = 0, \tag{5.8}$$

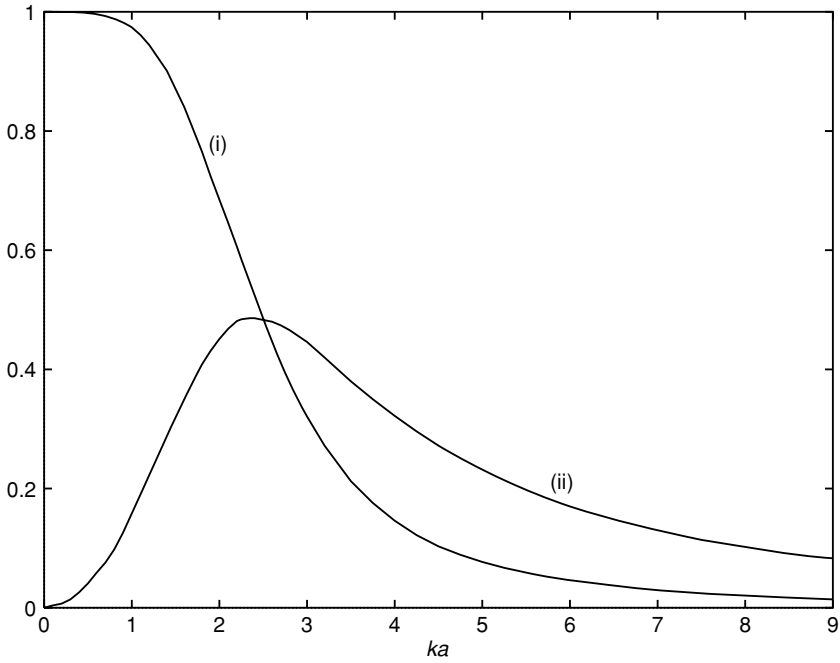

Figure 5.1 Coefficients in the volume flux Q: (i) $16F_1'(ka)/(ka)^3$, (ii) $8\{2F_2'(ka)/ka + 1\}/(ka)^2$.

together with

$$\bar{\tilde{v}}_z = \sum_{n=0}^{N} U_n \, \mathrm{e}^{-nt_0 s}, \quad \text{at} \quad r = a, \tag{5.9}$$

and a boundedness condition at $r = 0$. The solution of (5.8) with (5.9) for $\bar{\tilde{v}}_z$ is

$$\bar{\tilde{v}}_z = \frac{J_0\{\mathrm{i}r(s/\nu)^{1/2}\}}{J_0\{\mathrm{i}a(s/\nu)^{1/2}\}} \sum_{n=0}^{N} U_n \, \mathrm{e}^{-nt_0 s}.$$

As a consequence the transform of the volume flux of the unsteady part of the flow field is

$$\bar{Q} = 2\pi \int_0^a r\bar{\tilde{v}}_z \, \mathrm{d}r = -2\pi \mathrm{i}a \left(\frac{\nu}{s}\right)^{1/2} \frac{J_1\{\mathrm{i}a(s/\nu)^{1/2}\}}{J_0\{\mathrm{i}a(s/\nu)^{1/2}\}} \sum_{n=0}^{N} U_n \, \mathrm{e}^{-nt_0 s},$$

and from this, the instantaneous volume flux across any section is given by

$$Q = \frac{P\pi a^4}{8\mu} + \frac{2\pi a^4}{\nu}\frac{\partial}{\partial t}\left\langle \sum_{n=0}^{N} U_n \left[\frac{1}{2} - 2\sum_{m=1}^{\infty} \lambda_m^{-2} \times \exp\left\{ -\frac{\lambda_m^2 \nu}{a^2}(t - nt_0) \right\} \right] H(t - nt_0) \right\rangle,$$

where λ_m is the mth zero of J_0. If Q_0 is the volume flux for a single pulse then, when this has been established,

$$Q_0 = \frac{P\pi a^4}{8\mu} + 4\pi a^2 U_0 \sum_{m=1}^{\infty} \exp\left(-\frac{\lambda_m^2 \nu}{a^2} t \right). \tag{5.10}$$

From (5.10) it is seen that for a range of values of t, $0 < t < t_1$, $Q_0 < 0$ provided that

$$\frac{32 U_0 \mu}{P a^2} \sum_{m=1}^{\infty} \exp\left(-\frac{\lambda_m^2 \nu}{a^2} t \right) < -1,$$

that is, provided that the pulse strength is sufficiently large and negative. This consideration motivated, in part, the work of Lance at a time when it was thought that the firing of guns in certain combat aircraft might be the cause of fuel starvation.

5.1.4 The effects of suction or injection on periodic flow

In section 3.4.3 we considered the flow within a porous tube, in particular as studied by Terrill and Thomas (1969). Skalak and Wang (1977) have addressed this same problem, that is with uniform suction, or injection, with velocity V, at the boundary of the pipe, $r = a$, but now modified by the introduction of an oscillatory pressure gradient along it. Thus, for the pressure, we write

$$\frac{p - p_0}{\rho} = \frac{V^2}{R}\left(2f' - \frac{R}{2}\frac{f^2}{\eta} \right) + A\left(\frac{z}{a} \right)^2 + B\left(\frac{z}{a} \right) \mathrm{e}^{\mathrm{i}\omega t} \tag{5.11}$$

where, when compared with the steady case, we have set the uniform velocity U_0 to zero. With the velocity components

$$v_r = V\eta^{-1/2} f(\eta), \quad v_z = -2V\frac{z}{a} f'(\eta) + \frac{Ba}{4\nu} h(\eta)\, \mathrm{e}^{\mathrm{i}\omega t}, \tag{5.12}$$

where, as before, $\eta = (r/a)^2$. From (5.11) and (5.12) equation (1.21) gives, for $f(\eta)$, equation (3.35) with boundary conditions (3.36), and for $h(\eta)$,

$$\eta h'' + h' + \tfrac{1}{2}R(f'h - fh') - \mathrm{i}M^2 h = 1; \quad R = \frac{Va}{\nu}, \quad M^2 = \frac{\omega a^2}{4\nu}, \tag{5.13}$$

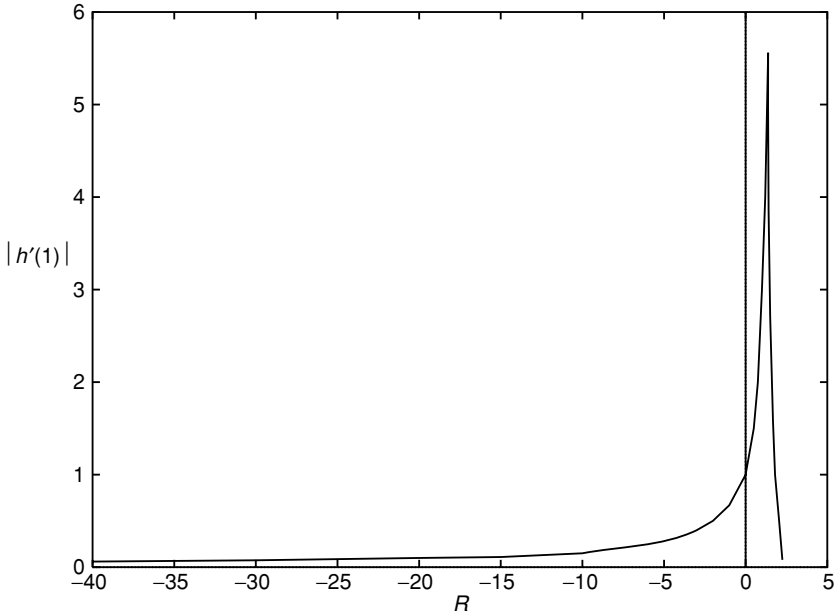

Figure 5.2 The variation of $|h'(1)|$ with R ($M^2 = 0.2$).

together with

$$\lim_{\eta \to 0}(\eta^{1/2} h') = h(1) = 0.$$

The solutions of (3.35), (3.36) for the steady case have been considered in chapter 3, and the complex nature of the solutions is illustrated in figure 3.9. For the unsteady case an additional parameter, M, is involved. Skalak and Wang have made a comprehensive survey of the solutions of (5.13) in (M, R)-parameter space. One of the more interesting features is for small M, and for the solution set I, a resonance type of phenomenon close to $R = 0$. This is illustrated in figure 5.2 where $|h'(1)|$ is plotted as a function of R for $M^2 = 0.2$.

Unsteady annular pipe flow with suction and injection has been considered by Wang (1971). With $v_r = V$ at $r = a$ and $v_r = Va/b$ at $r = b$, $b < a$, the radial component of velocity is simply $v_r = Va/r$, and with the pressure given by

$$\frac{p - p_0}{\rho} = \frac{\nu V a}{2r^2} - \frac{Pz}{\rho} + \frac{\bar{P}z}{\rho}\, \mathrm{e}^{\mathrm{i}\omega t},$$

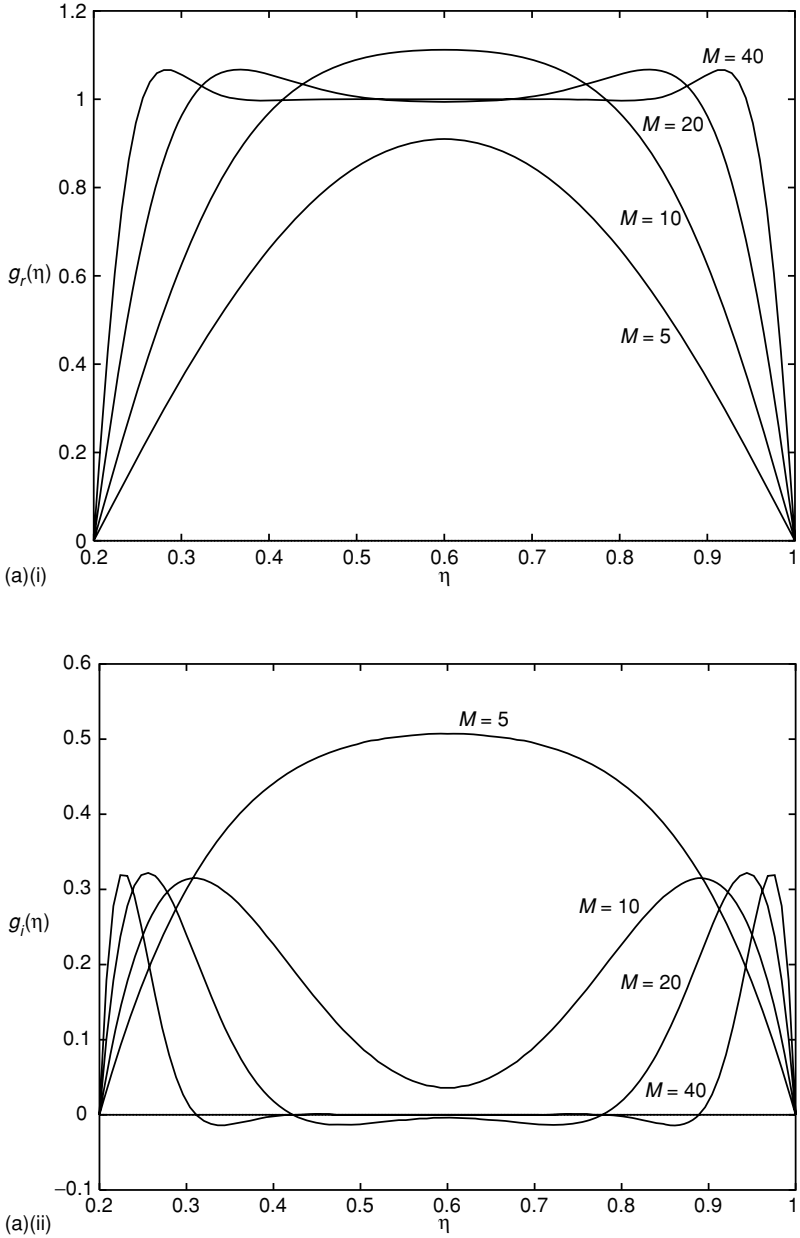

Figure 5.3 (a) Velocity profiles $g = g_r + \mathrm{i}g_i$ for various values of M with $R = 1$. (i) $g_r(\eta)$, (ii) $g_i(\eta)$. (b) As (a) with $R = -1$.

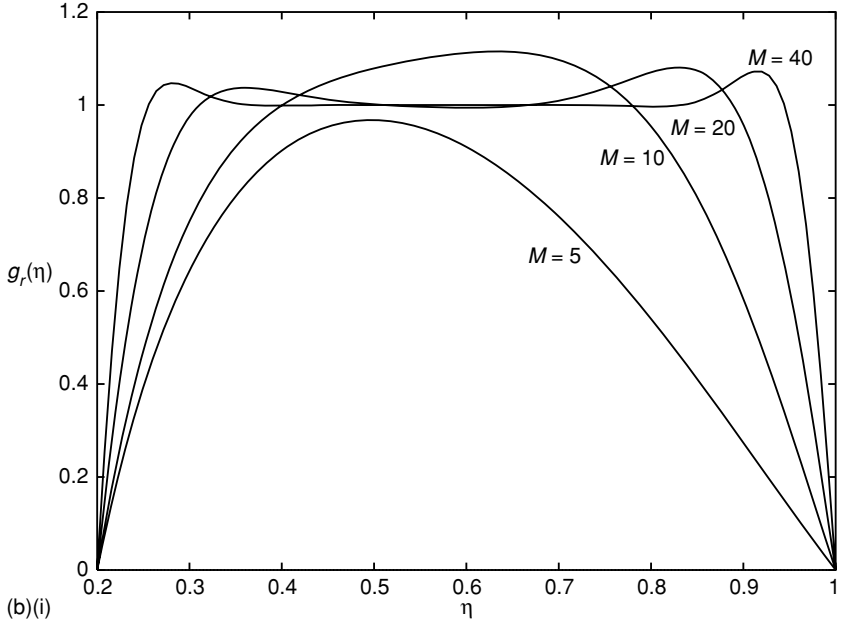

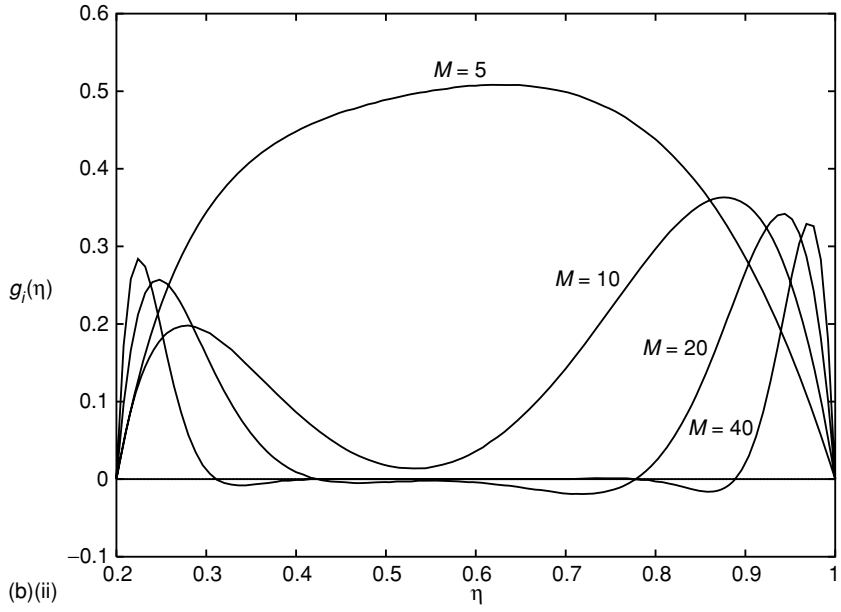

Figure 5.3 (*cont.*)

the axial component of velocity has the form

$$v_z = \{f(\eta) + g(\eta)\, e^{i\omega t}\}, \quad \eta = r/a. \tag{5.14}$$

The time-independent part of (5.14) has been discussed by Berman (1958a), and from (1.21) the equation for $g(\eta)$ is

$$g'' + \frac{1}{\eta}(1-R)g' - iM^2 g = \frac{\bar{P}a^2}{\mu V}, \quad \text{where now} \quad M^2 = \frac{\omega a^2}{\nu}. \tag{5.15}$$

An exact solution of equation (5.15), with $v_z = 0$ at $\eta = b/a$, 1 which we do not reproduce, involving Bessel functions of imaginary argument, has been obtained by Wang (1971). However, Wang notes that for the special cases $R = 1 - 2n$, where n is an integer, the general solution of (5.15) is

$$g(\eta) = \frac{i\bar{P}}{\rho\omega V} + C_1 \left(\frac{1}{\eta}\frac{d}{d\eta}\right)^n \exp\left\{-\frac{(1+i)}{\sqrt{2}} M\eta\right\} + C_2 \left(\frac{1}{\eta}\frac{d}{d\eta}\right)^n \exp\left\{\frac{(1+i)}{\sqrt{2}} M\eta\right\}.$$

In figure 5.3 we show representative velocity profiles for the cases $n = 0$, 1 and various values of M, with $b/a = 0.2$.

5.1.5 Pipes with varying radius

Uchida and Aoki (1977) and Skalak and Wang (1979) have considered the problem of a contracting or expanding pipe. The motivation for the investigation, in part anyway, is physiological with application to an understanding of flows associated with vascoconstriction, for example forced contractions and expansions of a valved vein or a thin bronchial tube. Both sets of authors consider contraction/expansion rates of the form $a(t) = a_0(1-\alpha t)^{1/2}$ where α may be positive (contraction) or negative (expansion). The similarity reductions differ slightly; following Skalak and Wang we write

$$\psi = \frac{\alpha a_0^2 z}{2} f(\eta) \quad \text{where} \quad \eta = \frac{r^2}{a_0^2(1-\alpha t)},$$

so that

$$v_r = -\frac{\alpha a_0 f(\eta)}{2(1-\alpha t)^{1/2}\eta^{1/2}} \quad \text{and} \quad v_z = \frac{\alpha z f'(\eta)}{(1-\alpha t)}.$$

The pressure p is given by

$$\frac{p_0 - p}{\rho} = \frac{\alpha^2 a_0^2}{4(1-\alpha t)}\left(\frac{\operatorname{sgn}\alpha}{M^2} f' + \frac{f^2}{2\eta} - f\right) - \frac{2\nu\alpha z^2 A}{a_0^2(1-\alpha t)^2},$$

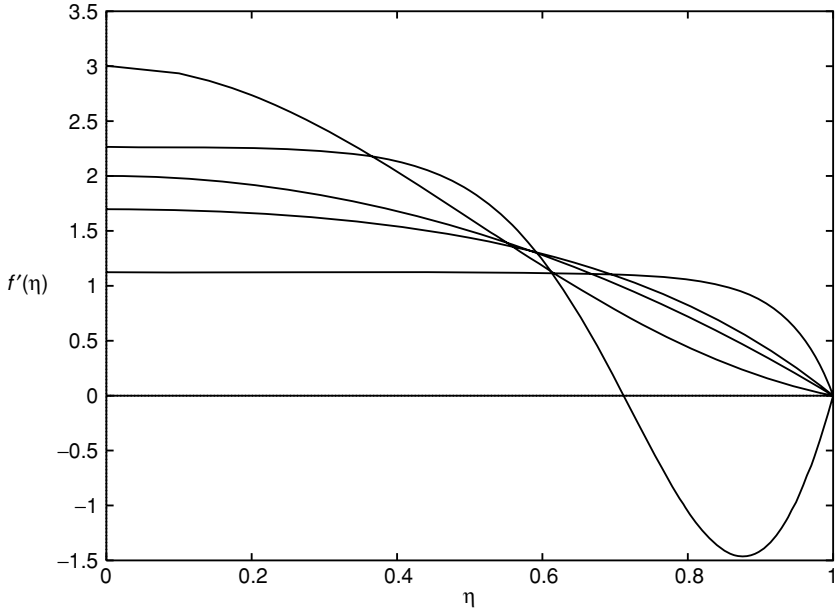

Figure 5.4 Velocity profiles within a contracting ($\alpha > 0$) and expanding ($\alpha < 0$) pipe for various values of M^2. At $\eta = 0$, from the lowest, we have $M^2 = 30.416$ ($\alpha > 0$), $M^2 = 0.86085$ ($\alpha > 0$), $M^2 = 0$, $M^2 = 6.22206$ ($\alpha < 0$), $M^2 = 0.73305$ ($\alpha < 0$).

where A is a constant and p_0 may depend upon t, and equation (1.21) yields, as the equation for $f(\eta)$,

$$\eta f''' + f'' - \operatorname{sgn}\alpha M^2(\eta f'' + f' + f'^2 - ff'') = A$$

where $M^2 = a_0^2|\alpha|/4\nu$, together with boundary conditions

$$\lim_{\eta\to 0}(\eta^{-1/2} f) = 0, \quad \lim_{\eta\to 0}(\eta^{1/2} f'') = 0$$

which express symmetry of the solution about the pipe centre-line $r = 0$, and

$$f'(1) = 0, \quad f(1) = 1$$

which, respectively, represent no slip at the pipe wall and no flow through it. The constant A is determined as part of the solution procedure as $A = -\operatorname{sgn}\alpha M^2\{f'(0) + f'(0)^2\}$.

In figure 5.4 velocity profiles, for various values of M^2 for both expanding and contracting pipes, are presented.

Typical of the 'squeezing' flows ($\alpha > 0$) is the development of boundary layers at the pipe boundary as M increases. For $\alpha < 0$ flow reversal is encountered as M increases, with outflow occurring close to the pipe wall.

In the above, the radial boundary motion is unidirectional. Blyth, Hall and Papageorgiu (2003) have addressed the problem of flow within the pipe when its radius varies in a time-oscillatory manner. Suppose that we now write

$$\psi = \nu z f(\eta, t) \quad \text{where} \quad \eta = \frac{r}{a(t)} \tag{5.16}$$

then, since the vorticity has the single component $-(\partial v_z/\partial r)\hat{\boldsymbol{\theta}}$, equation (1.7) gives, for f,

$$\frac{a^2}{\nu}\left(f_{\eta\eta t} - \frac{f_{\eta t}}{\eta}\right) = \eta\left(\frac{f_\eta}{\eta}\right)_{\eta\eta\eta} + \left(\frac{3a}{\nu}\frac{\mathrm{d}a}{\mathrm{d}t} - \frac{1}{\eta^2}\right) f_\eta + \left(1 + f + \frac{a}{\nu}\frac{\mathrm{d}a}{\mathrm{d}t}\eta^2\right)\left(\frac{f_\eta}{\eta}\right)_{\eta\eta} + \left(\frac{f_\eta}{\eta} - f_{\eta\eta}\right)\frac{f_\eta}{\eta}, \tag{5.17}$$

with boundary conditions

$$\lim_{\eta\to 0}(\eta^{-1} f) = \lim_{\eta\to 0}(\eta^{-1} f_\eta)_\eta = 0; \quad f(1) = -\frac{a}{\nu}\frac{\mathrm{d}a}{\mathrm{d}t}, \quad f_\eta(1) = 0. \tag{5.18}$$

It is clear from (5.17) and (5.18) that complete self-similarity is obtained only when $a\,\mathrm{d}a/\mathrm{d}t =$ constant and $\partial f/\partial t = 0$, which corresponds to the case considered by Uchida and Aoki, and Skalak and Wang, treated above. The formulation (5.16) has, however, resulted in a reduction by one of the independent variables. Blyth *et al.* treat, in detail, the case $a(t) = a_0(1 + \Delta\cos\omega t), 0 < \Delta < 1$. A practical reason for this choice is to understand further the physiological application of transmyocardial laser revascularisation that had earlier been partly modelled and analysed by Waters (2001). With the parameter $M^2 = \omega a_0^2/\nu$ numerical solutions of (5.17) and (5.18) have been obtained, revealing complex dynamics. For small M the flow and forcing are synchronous, and as M increases a Hopf bifurcation occurs. As M increases further the dynamics depend upon Δ. For small Δ the Hopf bifurcation leads to quasi-periodic solutions. At intermediate values of Δ the solutions tend to a chaotic attractor at large t. For larger values of Δ the solution remains periodic as M increases with intervals of integer multiples of the driving period emerging.

5.1.6 Impulsive cylinder flows

The flow induced by a solid cylinder set into a 'sliding' motion parallel to its generators has been considered by several authors. Suppose that the cylinder

surface is porous, and at it a velocity of suction $v_r|_{r=a} = -V$ is applied, and let the cylinder be set into motion with speed $w_0(t)$. Then if in the resulting motion $v_z = v_z(r, t)$ we have $v_r = -Va/r$ and, from equation (1.21), the equation for v_z is

$$\frac{\partial v_z}{\partial t} = \nu \left\{ \frac{\partial^2 v_z}{\partial r^2} + \frac{(1+R)}{r} \frac{\partial v_z}{\partial r} \right\} \quad \text{where} \quad R = \frac{Va}{\nu}, \tag{5.19}$$

with

$$v_z = 0, t = 0, r > a; \quad v_z = w_0(t), t > 0, r = a; \quad v_z \to 0 \text{ as } r \to \infty.$$

Laplace transform techniques yield as the solution of equation (5.19), with its attendant boundary conditions,

$$v_z(r, t) = \frac{1}{2\pi \mathrm{i}} \left(\frac{a}{r}\right)^{R/2} \int_{c-\mathrm{i}\infty}^{c+\mathrm{i}\infty} \mathrm{e}^{st} \frac{K_{R/2}\left(r\sqrt{s/\nu}\right)}{K_{R/2}\left(a\sqrt{s/\nu}\right)} \bar{w}_0(s)\, \mathrm{d}s, \tag{5.20}$$

where $K_{R/2}$ is a modified Bessel function of the second kind and

$$\bar{w}_0(s) = \int_0^\infty \mathrm{e}^{-st} w_0(t)\, \mathrm{d}t.$$

The formal solution (5.20) was given by Irmay and Zuzovsky (1970) for the case $R = 0$. For constant sliding velocity, with $w(t) = W$ for $t > 0$, so that $\bar{w}_0 = s^{-1}$, Hasimoto (1956) derives from (5.20) the solution

$$v_z(r, t) = W \left\{ \left(\frac{a}{r}\right)^R + \frac{2}{\pi} \left(\frac{a}{r}\right)^{R/2} \times \int_0^\infty \frac{\mathrm{e}^{-\nu\sigma^2 t}}{\sigma} \left(\frac{J_{R/2}(\sigma r) Y_{R/2}(\sigma a) - J_{R/2}(\sigma a) Y_{R/2}(\sigma r)}{J_{R/2}^2(\sigma a) + Y_{R/2}^2(\sigma a)} \right) \mathrm{d}\sigma \right\}, \tag{5.21}$$

a solution also given for the case $R = 0$ by Batchelor (1954) by analogy with the corresponding heat-conduction problem of a circular cylinder whose temperature is suddenly raised to a uniform value (see Carslaw and Jaeger (1947)). Batchelor shows, in particular, that for the shear stress at the cylinder

$$\mu \frac{\partial v_z}{\partial r}\bigg|_{r=a} \sim -\left(\frac{\rho\mu}{\pi t}\right)^{1/2} W \quad \text{as} \quad t \to 0.$$

This result coincides with that for the classical impulsive flat plate problem considered in section 4.2, as may be expected when $t \ll a^2/\nu$.

Hasimoto has observed that considerable simplifications of (5.21) may be achieved for values of $R = -1 + 2n$, where n is an integer. For example

with $R = -1$, which corresponds to transpiration across the cylinder surface:

$$v_z = W\operatorname{erfc}\left\{\frac{r-a}{2(\nu t)^{1/2}}\right\} \quad \text{so that} \quad v_z \to W \quad \text{as} \quad t \to \infty \quad \text{for any fixed} \quad r.$$

For the suction case $R = 1$:

$$v_z = \frac{aW}{r}\operatorname{erfc}\left\{\frac{r-a}{2(\nu t)^{1/2}}\right\} \quad \text{so that} \quad v_z \sim \frac{aW}{r} \quad \text{as} \quad t \to \infty \quad \text{for any fixed} \quad r.$$

In a not unrelated problem Lagerstrom and Cole (1955) have considered problems in which the cylinder expands radially with radius $a(t) = At^n$, and again slides parallel to its generators with speed W. In particular they find an exact solution for $n = \frac{1}{2}$. In that case, with $a(t) = a_0(Wt/a_0)^{1/2}$ where a_0 is a constant, the continuity equation $\partial(rv_r)/\partial r = 0$ with $v_r = \mathrm{d}a/\mathrm{d}t$ at $r = a$ gives

$$v_r = \frac{a}{r}\frac{\mathrm{d}a}{\mathrm{d}t} = \frac{a_0 W}{2r}. \tag{5.22}$$

With $v_z = v_z(r, t)$ the momentum equation (1.21) is then

$$\frac{\partial v_z}{\partial t} = \nu\left\{\frac{\partial^2 v_z}{\partial r^2} + \frac{1}{r}\left(1 - \frac{R}{2}\right)\frac{\partial v_z}{\partial r}\right\}, \quad R = \frac{Wa_0}{\nu}, \tag{5.23}$$

which may be compared with equation (5.19). The boundary conditions now require

$$v_z = 0, t = 0, r > 0; v_z = W, t > 0, r = a_0\left(\frac{Wt}{a_0}\right)^{1/2}; \; v_z \to 0 \text{ as } r \to \infty.$$

A similarity solution is available by writing $v_z(r, t) = Wf(\eta)$ where $\eta = r/2(\nu t)^{1/2}$ so that f satisfies

$$\eta f'' + \left(1 - \tfrac{1}{2}R + 2\eta\right)f' = 0, \quad f(\sqrt{R}/2) = 1, \quad f(\infty) = 0;$$

with solution

$$f(\eta) = \int_\eta^\infty \mathrm{e}^{-\sigma^2}\sigma^{R/2-1}\mathrm{d}\sigma \Big/ \int_{\sqrt{R}/2}^\infty \mathrm{e}^{-\sigma^2}\sigma^{R/2-1}\mathrm{d}\sigma. \tag{5.24}$$

As in the previous example the expression (5.24) simplifies for particular values of the Reynolds number R, namely $R = 2n$ for integer n. For example with $R = 2, 4$ we have, respectively,

$$v_z = W\frac{\operatorname{erfc}\eta}{\operatorname{erfc}(1/\sqrt{2})}, \quad v_z = W\mathrm{e}^{(1-\eta^2)}.$$

In this original formulation the expanding cylinder has $r = 0$ at $t = 0$. For a slight generalisation write $a(t) = a_0\{(Wt + a_0)/a_0\}^{1/2}$, $t > 0$ so that at $t = 0$, $a(0) = a_0$. With $\eta = r/2\{\nu(t + a_0/W)\}^{1/2}$ the solution (5.24) is unchanged.

In the above examples the cylinder in motion has been of circular cross-section. Tranter (1951) has considered the case of an impermeable cylinder of elliptic cross-section set into uniform motion at the initial instant parallel to its generators. A formal solution is obtained by introducing elliptic co-ordinates, which coincides with Batchelor's solution in the limit as the ellipse axis ratio approaches unity.

In addition to impulsive sliding flows, an exact solution is available for the case in which a circular cylinder of radius a is set into motion with uniform angular velocity V/a. With $v_\theta = v_\theta(r, t)$ equation (1.20) gives

$$\frac{\partial v_\theta}{\partial t} = \nu\left(\frac{\partial^2 v_\theta}{\partial r^2} + \frac{1}{r}\frac{\partial v_\theta}{\partial r} - \frac{v_\theta}{r^2}\right), \tag{5.25}$$

together with

$$v_\theta = 0, r > a, t = 0; \quad v_\theta = V, r = a, t > 0; \quad v_\theta \to 0 \text{ as } r \to \infty, t \geq 0.$$

The solution of the Laplace transform of (5.25) is again readily obtained, and was given by Lagerstrom (1996) as

$$\bar{v}_\theta = \frac{V}{2\pi \mathrm{i}} \int_{c-\mathrm{i}\infty}^{c+\mathrm{i}\infty} \frac{\mathrm{e}^{st}}{s} \frac{K_1\left(r\sqrt{s/\nu}\right)}{K_1\left(a\sqrt{s/\nu}\right)} \mathrm{d}s. \tag{5.26}$$

The inverse of (5.26) is

$$v_\theta = V\left\{\frac{a}{r} + \frac{2}{\pi}\int_0^\infty \frac{\mathrm{e}^{-\nu\sigma^2 t}}{\sigma}\left(\frac{J_1(\sigma r)Y_1(\sigma a) - J_1(\sigma a)Y_1(\sigma r)}{J_1^2(\sigma a) + Y_1^2(\sigma a)}\right)\mathrm{d}\sigma\right\}. \tag{5.27}$$

The similarity between these Rayleigh-type sliding and rotating flows is evidenced by a comparison of equations (5.21) and (5.27).

Oscillatory flows, the analogue of Stokes' problem for the oscillating flat plate discussed in chapter 4, also admit exact solutions for the circular cylinder of radius a. Consider first the situation in which an impermeable cylinder performs an oscillatory motion parallel to its generators such that at $r = a$, $v_z = W\,\mathrm{e}^{\mathrm{i}\omega t}$. Equation (5.19), with $R \equiv 0$, is the equation satisfied by $v_z(r, t)$ with solution

$$v_z = W\frac{K_0\left\{r(\mathrm{i}\omega/\nu)^{1/2}\right\}}{K_0\left\{a(\mathrm{i}\omega/\nu)^{1/2}\right\}}\,\mathrm{e}^{\mathrm{i}\omega t}. \tag{5.28}$$

Far from the cylinder equation (5.28) gives

$$v_z \sim Cr^{-1/2} \exp\{-(\omega/2\nu)^{1/2} r\} \exp[\mathrm{i}\{\omega t - (\omega/2\nu)^{1/2} r\}] \quad \text{as} \quad r \to \infty, \tag{5.29}$$

which represents a decaying viscous wave as in the two-dimensional Stokes solution but with the decay rate now enhanced by a factor $r^{-1/2}$ reflecting the change of geometry. Hasimoto (1956) has also addressed this problem when suction is applied at the cylinder surface.

When the cylinder performs torsional oscillations with angular velocity $(V/a)\,\mathrm{e}^{\mathrm{i}\omega t}$ equation (5.25) is satisfied by v_θ with solution, for the cylinder assumed impermeable,

$$v_\theta = V \frac{K_1\left\{r(\mathrm{i}\omega/\nu)^{1/2}\right\}}{K_1\left\{a(\mathrm{i}\omega/\nu)^{1/2}\right\}} \mathrm{e}^{\mathrm{i}\omega t},$$

which also exhibits the behaviour (5.29) as $r \to \infty$.

5.2 Beltrami flows and their generalisation

As we have noted in earlier chapters, Beltrami flows are those for which $\mathbf{v} \wedge \boldsymbol{\omega} \equiv \mathbf{0}$ and it was shown, in particular, in section 4.6 that there can be no such unsteady flows that are axisymmetric. For their generalisation, with $\nabla \wedge (\mathbf{v} \wedge \boldsymbol{\omega}) \equiv \mathbf{0}$, $\boldsymbol{\omega}$ satisfies equation (4.39), the solution of which for axisymmetric flows does not appear to have attracted close attention. However, Irmay and Zuzovsky (1970) have presented one such solution for which the stream function is given as

$$\psi = -(c_1 + c_2 z)\,\mathrm{e}^{-r^2/4\nu t},$$

where c_1, c_2 are constants, so that

$$v_r = \frac{c_2}{r}\,\mathrm{e}^{-r^2/4\nu t}, \quad v_z = \frac{c_1 + c_2 z}{2\nu t}\,\mathrm{e}^{-r^2/4\nu t} \quad \text{and} \quad \boldsymbol{\omega} = \frac{(c_1 + c_2 z) r}{4\nu^2 t^2}\,\mathrm{e}^{-r^2/4\nu t}\hat{\boldsymbol{\theta}}. \tag{5.30}$$

From (5.30) it is seen that at $t = 0$ the fluid is everywhere at rest. For $t > 0$ a radial flow develops from the axis $r = 0$, together with an axial flow induced by an appropriate pressure gradient. As $t \to \infty$, $v_z \to 0$ for $r > 0$, and the flow becomes the irrotational flow due to a line source on the axis $r = 0$.

5.3 Stagnation-point flows

As for the unsteady two-dimensional problems considered in chapter 4 there are unsteady axisymmetric, and indeed three-dimensional, exact solutions of the Navier–Stokes equations constructed by superposing a time-dependent motion,

typically a fluctuation, upon a known steady solution. We begin by considering such a case.

5.3.1 The Homann flow against an oscillating plate

Weidman and Mahalingham (1997) consider the axisymmetric stagnation-point flow against a porous plane boundary at which the transpiration velocity is a constant, equal to $-W_0$, and which performs periodic oscillations in its own plane, in the x-direction, with frequency ω. With rectangular co-ordinates (x, y, z) the velocity components may be written as

$$u = kxf'(\eta) + U_0 g(\eta)\, \mathrm{e}^{\mathrm{i}\omega t}, \quad v = kyf'(\eta), \quad w = -2(k\nu)^{1/2} f(\eta) - W_0, \qquad \eta = \left(\frac{k}{\nu}\right)^{1/2} z, \tag{5.31}$$

and the pressure as

$$\frac{p - p_0}{\rho} = -\frac{1}{2}k^2(x^2 + y^2) - 2k\nu\{f^2(\eta) + f'(\eta)\} - 2(k\nu)^{1/2} W_0. \tag{5.32}$$

In equation (5.31) k is again the constant strain rate with U_0/ω the amplitude of the plate oscillations. As in the two-dimensional case the pressure is unaffected by the oscillatory component of velocity. This is evident when comparing (5.32) with equation (3.20) where the difference is accounted for by the suction velocity imposed at the boundary. The velocity field (5.31) satisfies the continuity equation (1.12) and equations (1.10) and (1.11) are satisfied identically provided that f, g satisfy the ordinary differential equations

$$f''' + 2ff'' + Sf'' - f'^2 + 1 = 0, \tag{5.33}$$

$$g'' + 2fg' + Sg' - f'g + \mathrm{i}\Omega g = 0, \tag{5.34}$$

where $S = W_0/(k\nu)^{1/2}$ and $\Omega = \omega/k$. The boundary conditions require

$$f(0) = f'(0) = 0, \quad f'(\infty) = 1; \quad g(0) = 1, \quad g(\infty) = 0. \tag{5.35}$$

There are special cases: (a) $U_0 = S = 0$, which corresponds to the classical steady, axisymmetric stagnation-point flow of Homann (1936), (b) $\Omega = S = 0$, which represents the case of a flat plate moving transversely at uniform speed U_0 beneath the axisymmetric stagnation-point flow as considered by Wang (1973) and (c) $S = 0$, representing the stagnation-point flow towards an impermeable plate performing transverse oscillations.

Weidman and Mahalingam have integrated the system (5.33) to (5.35) numerically for a wide range of values of the parameters S and Ω, and have in

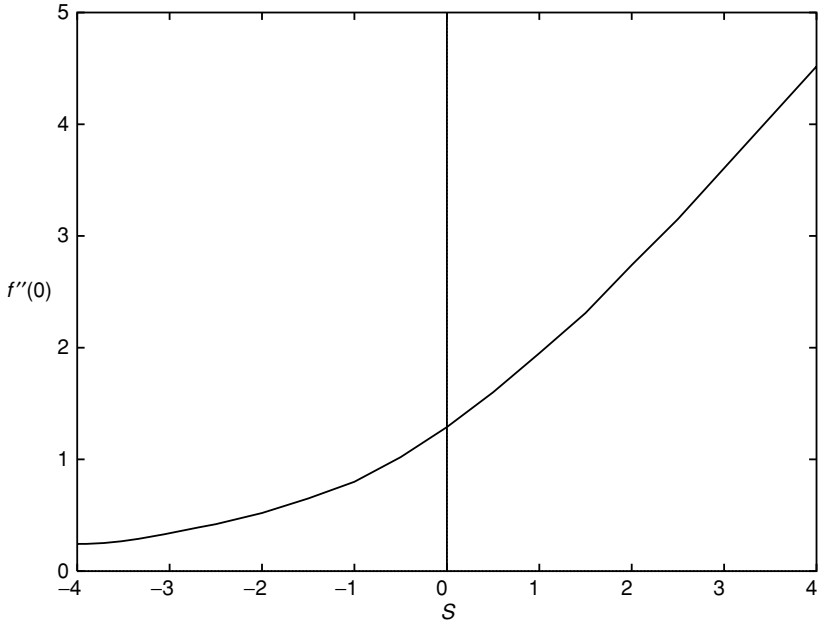

Figure 5.5 The variation of the radial shear-stress parameter $f''(0)$ with S.

addition carried out asymptotic analyses for large $|S|$, Ω. The shear stress on the oscillating plate is given by

$$\boldsymbol{\tau} = \rho k^{3/2}\nu^{1/2} r f''(0)\hat{\mathbf{r}} + \rho U_0 (k\nu)^{1/2} |g'(0)|\, \mathrm{e}^{\mathrm{i}(\omega t+\phi)}\mathbf{i}$$

where $r = (x^2 + y^2)^{1/2}$ and $\phi = \arg\{g'(0)\}$. Thus, the shear stress has a steady radial component and an unsteady component along the direction of the plate oscillation. In figure 5.5 the dependence of $f''(0)$ upon the transpiration parameter S is shown. As the suction increases so the shear stress increases. For negative values of S, which corresponds to blowing from the plate, the time-independent part of the solution is essentially that of opposing stagnation-point flow with a free stagnation point. The stand–off distance of this point increases with the blowing rate as shown in figure 5.6. For each value of Ω, $|g'(0)|$ also increases as S increases as can be seen in figure 5.7, where $|g'(0)|$ is shown as a function of Ω for discrete values of S. For each value of S, $|g'(0)|$ is seen to increase monotonically with Ω, consistent with the two-dimensional flow discussed in chapter 4. The phase angle ϕ also increases with Ω, for each value of S, as shown in figure 5.8; Weidman and Mahalingam demonstrate that, for all S, $\phi \to \pi/4$ as $\Omega \to \infty$.

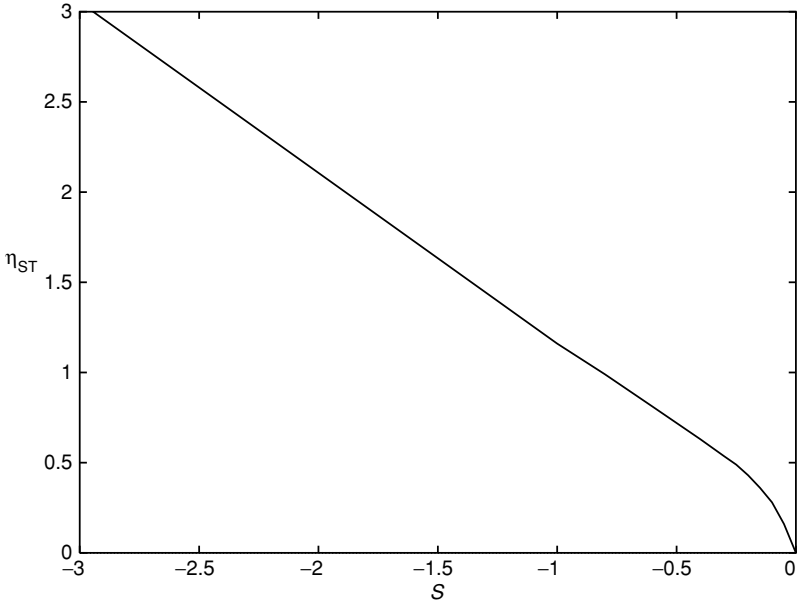

Figure 5.6 The stand-off distance η_{ST} of the free stagnation point as a function of the blowing rate S.

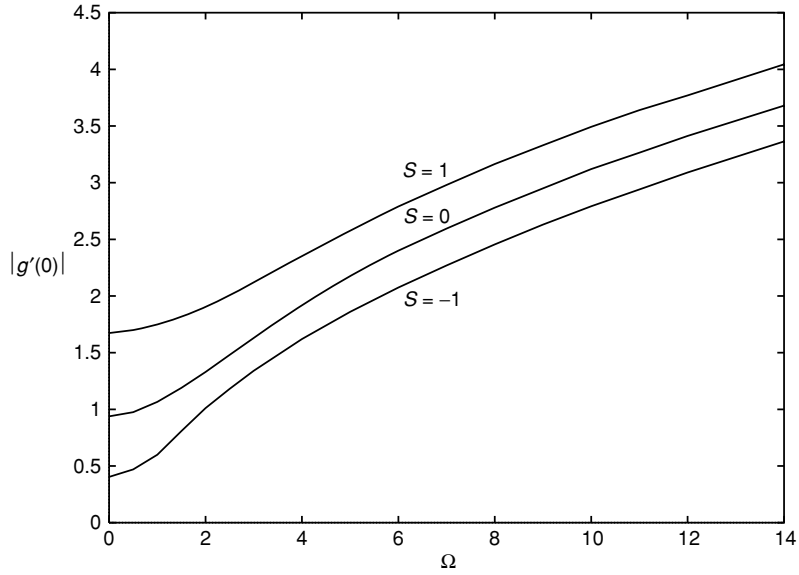

Figure 5.7 The transverse shear-stress parameter $|g'(0)|$ as a function of Ω for various values of S.

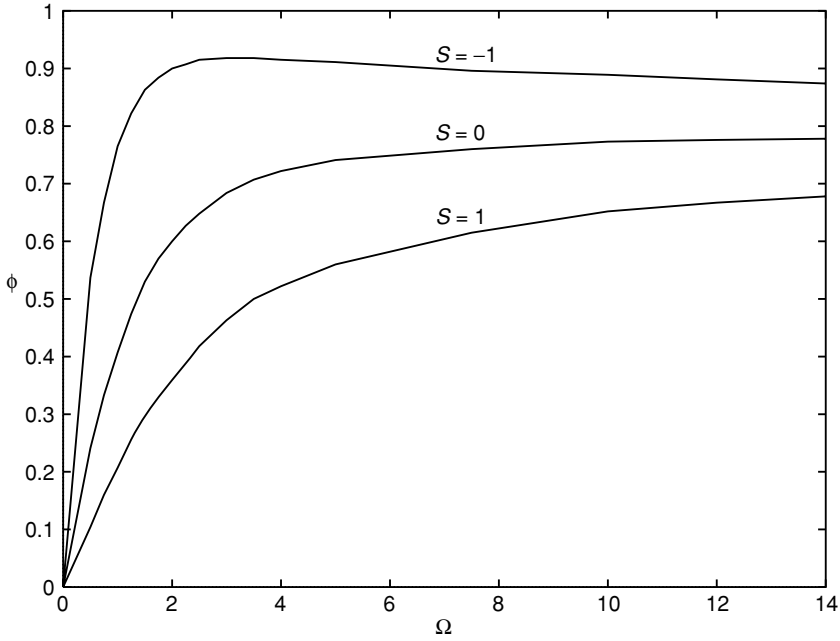

Figure 5.8 The phase angle ϕ as a function of Ω for various values of S.

5.3.2 Oblique stagnation-point flow

In section 4.7.4 we considered the unsteady three-dimensional stagnation-point flow of Cheng *et al.* (1971), where the parameter r ($0 \leq r \leq 1$) characterises the flow in the sense that for $r = 0$ the flow is two-dimensional, whilst for $r = 1$ an axisymmetric flow is recovered. Wang (1985b) has generalised this solution by introducing a time-dependent cross-flow, in the x-direction, of uniform shear. Although Wang formulates the problem in the general form of Cheng *et al.*, attention is focused upon the case $r = 1$. Following Wang we write

$$u = k\left\{\frac{xf'(\eta)}{1-kt} + \left(\frac{\nu}{k}\right)^{1/2}\frac{\gamma g(\eta)}{(1-kt)^{1/2}}\right\}, \quad v = k\frac{yf'(\eta)}{1-kt},$$
$$w = -2k\left(\frac{\nu}{k}\right)^{1/2}\frac{f(\eta)}{(1-kt)^{1/2}}, \tag{5.36}$$

where $\eta = (k/\nu)^{1/2}\, z/(1-kt)^{1/2}$, and the pressure as

$$\frac{p-p_0}{\rho} = -\frac{k^2(x^2+y^2)}{(1-kt)^2} + \frac{\gamma(\nu k^3)^{1/2}}{2(1-kt)^{3/2}}(3B-4A)x$$
$$+ \frac{\nu k}{(1-kt)}\{\eta f(\eta) - 2f^2(\eta) - 2f'(\eta)\}. \tag{5.37}$$

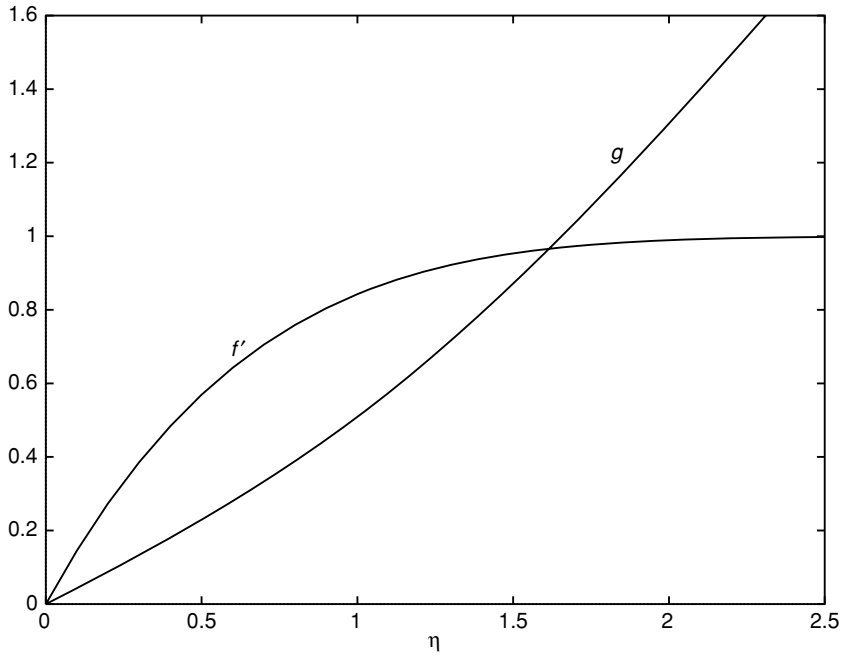

Figure 5.9 The velocity profiles $f'(\eta)$, $g(\eta)$ for the case $B = 4A/3$.

In this expression for the pressure, (5.37), the constant A is determined from the displacement of the basic onset flow, that is $A = \lim_{\eta\to\infty}(\eta - f)$. The constant B is arbitrary, but in turn determines the displacement of the cross-flow, such that $B = \lim_{\eta\to\infty}(\eta - g)$. Wang considers in detail the case for which $B = 4A/3$. With the equation of continuity satisfied identically, equations (1.9) and (1.10) give, using (5.36) and (5.37), as equations for $f(\eta)$ and $g(\eta)$,

$$f''' - \tfrac{1}{2}\eta f'' + 2ff'' - f'^2 - f' + 2 = 0,$$

$$g'' - \tfrac{1}{2}\eta g' + 2fg' - f'g - \tfrac{1}{2}g = 0,$$

with boundary conditions

$$f(0) = f'(0) = g(0) = 0; \qquad f'(\infty) = g'(\infty) = 1.$$

From the solution of these equations the profiles $f'(\eta)$, $g(\eta)$ are shown in figure 5.9.

The components of shear stress at the plate are given by

$$\tau_x = \mu \frac{\partial u}{\partial z}\bigg|_{z=0} = (\rho\mu k^3)^{1/2} \left\{ \frac{x f''(0)}{(1-kt)^{3/2}} + \left(\frac{\nu}{k}\right)^{1/2} \frac{\gamma g'(0)}{(1-kt)^{1/2}} \right\},$$

$$\tau_y = \mu \frac{\partial v}{\partial z}\bigg|_{z=0} = (\rho\mu k^3)^{1/2} \frac{y f''(0)}{(1-kt)^{3/2}}.$$

The vanishing of these two components determines the stagnation point of attachment as, with $f''(0) = 1.5570332$, $g'(0) = 0.4401276$,

$$x_s = -\gamma \left(\frac{\nu}{k}\right)^{1/2} \frac{g'(0)}{f''(0)}(1-kt) = -0.2827\gamma \left(\frac{\nu}{k}\right)^{1/2} (1-kt), \quad y_s = 0,$$

which approaches the origin as the singular time $t = k^{-1}$ is approached.

5.3.3 Unsteady stagnation on a circular cylinder

In section 3.4.2 the problem of stagnation flow on a circle of radius a circumscribing a cylinder of the same radius, with generators in the z-direction, was presented. If such a cylinder performs torsional oscillations with angular velocity $(V/a)\,\mathrm{e}^{\mathrm{i}\omega_1 t}$ and, simultaneously, longitudinal oscillations with speed $W\mathrm{e}^{\mathrm{i}\omega_2 t}$ then, when this is embedded within the steady 'circular' stagnation flow, an exact solution of the three-dimensional Navier–Stokes equations is available with, in cylindrical polar co-ordinates, velocity components given by

$$v_r = -ka\eta^{-1/2} f(\eta), \quad v_\theta = V\eta^{-1/2} g(\eta)\,\mathrm{e}^{\mathrm{i}\omega_1 t}, \quad v_z = 2kzf'(\eta) + Wh(\eta)\,\mathrm{e}^{\mathrm{i}\omega_2 t}, \tag{5.38}$$

where $\eta = (r/a)^2$, and pressure as

$$\frac{p-p_0}{\rho} = -2k^2z^2 - \frac{1}{2}k^2a^2\eta^{-1} f^2(\eta) - 2\nu k f'(\eta) + \frac{1}{2}V^2 \int_1^\eta (|g(s)|/s)^2\, \mathrm{e}^{2\mathrm{i}(\omega_1 t+\phi)}\, \mathrm{d}s, \tag{5.39}$$

where $\phi(\eta) = \arg\{g(\eta)\}$. If, in (5.38), we set $V \equiv 0$ then the flow is the analogue of the two-dimensional flow considered by Glauert (1956) and Rott (1956) in which, at a two-dimensional stagnation point, the flat plate oscillates orthogonal to the stagnation line, whilst if W is set to zero the resulting flow is the analogue of Rott's (1956) solution where the plate oscillates along the stagnation line.

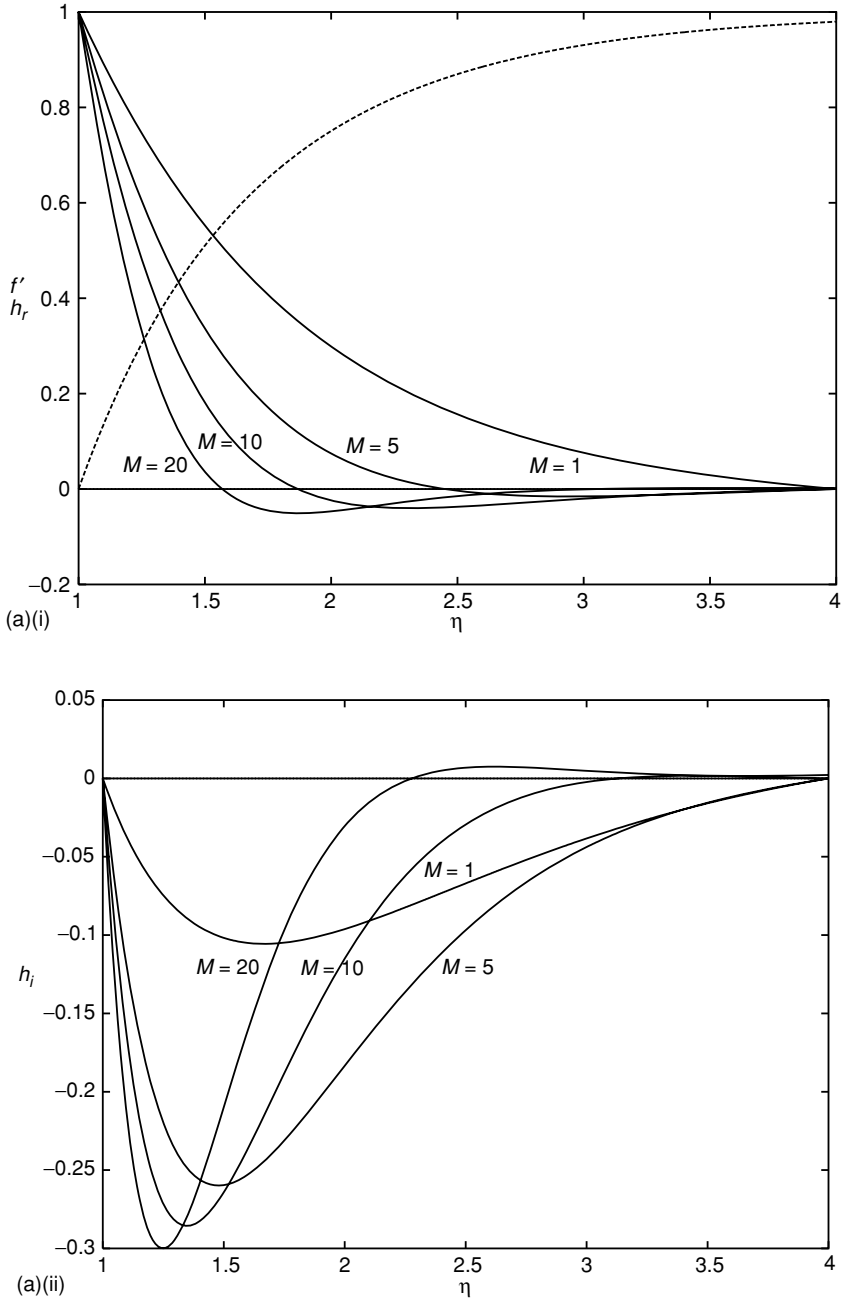

Figure 5.10 (a) Velocity profiles $f'(\eta)$ (broken line) and $h = h_r + \mathrm{i}h_\mathrm{i}$ for various values of M with $R = 1$. (i) $h_r(\eta)$, (ii) $h_i(\eta)$. (b) As (a) with $R = 10$.

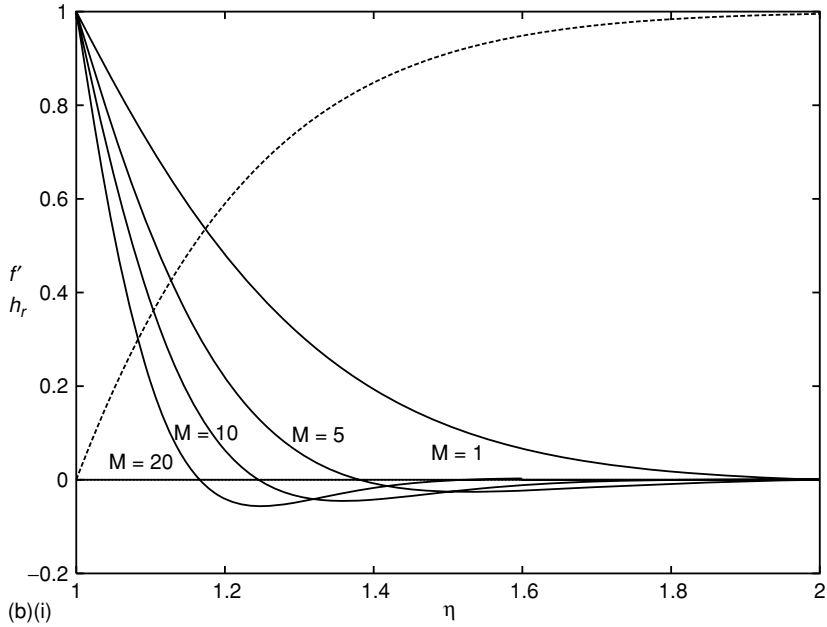

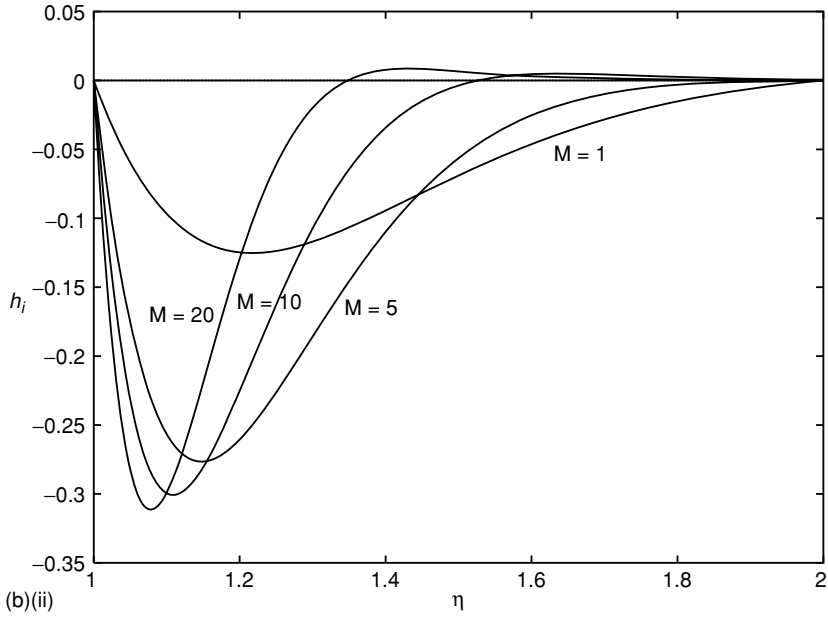

Figure 5.10 (*cont.*)

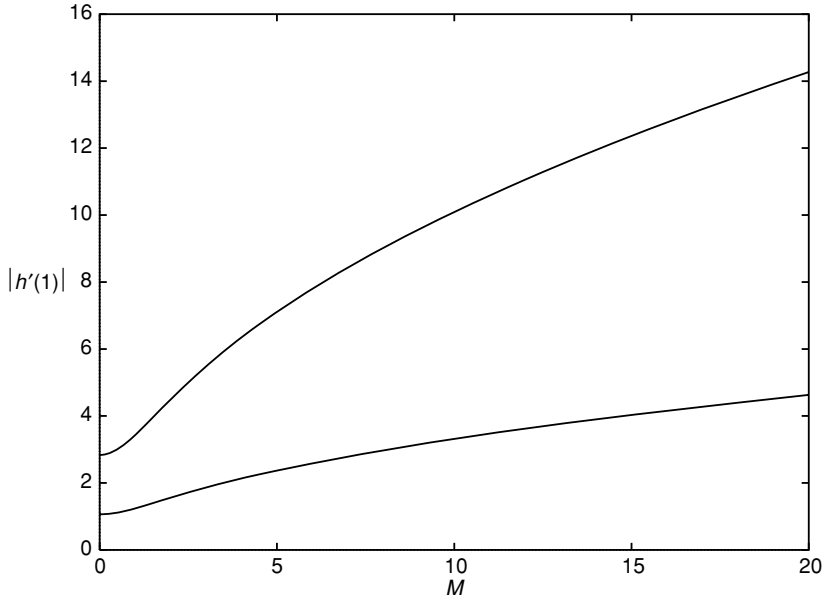

Figure 5.11 Variation of the shear-stress parameter $|h'(1)|$ with M for the two Reynolds numbers $R = 1$ (lower) and $R = 10$ (upper).

With the velocity field and pressure as in equations (5.38) and (5.39), equation (1.22) is satisfied identically whilst (1.19), (1.20) and (1.21) will be satisfied provided that $f(\eta)$, $g(\eta)$ and $h(\eta)$ satisfy the following ordinary differential equations,

$$\eta f''' + f'' + R(ff'' - f'^2 + 1) = 0, \quad f(1) = f'(1) = 0, \quad f'(\infty) = 1;$$

$$\eta g'' + R(fg' - \mathrm{i}M_1 g) = 0, \quad g(1) = 1, \quad g(\infty) = 0;$$

$$\eta h'' + h' + R(fh' - f'h - -\mathrm{i}M_2 h) = 0, \quad h(1) = 1, \quad h(\infty) = 0.$$

In these equations $R = ka^2/2\nu$ is a Reynolds number and $M_i = \omega_i/2k$ $(i = 1, 2)$. The special case $V \equiv 0$ has been considered by Gorla (1979) who determines solutions in the range $10^{-2} \leq R \leq 10^2$ for various values of M_2. In figure 5.10 we show representative velocity profiles for two values of the Reynolds number, whilst in figure 5.11 the variation of $|h'(1)|$ with M_2 is shown.

5.4 Squeeze flows

The unsteady squeezing of a viscous fluid between two parallel disks provides a model for the loading of mechanical parts as, for example, in a thrust bearing, or

for the draining of a fluid layer from between the two planes as in the draining of squeeze films between electrically or thermally conducting surfaces. For axisymmetric flow the fluid motion between the two disks, a distance $h(t)$ apart with $h_0 = h(0)$, has the nature of a double axisymmetric stagnation-point flow. In that case, using cylindrical polar co-ordinates and assuming that the origin is located on the lower disk which is assumed to be fixed, if we write $\psi = -Ur^2F(z,t)$ with U a typical velocity then

$$v_r = Ur\frac{\partial F}{\partial z} \quad \text{and} \quad v_z = -2UF. \tag{5.40}$$

The continuity equation is satisfied identically and equations (1.19) and (1.21) yield for the unknown F, and the pressure p

$$\frac{1}{R}F_{\eta\eta\eta} + 2FF_{\eta\eta} - F_\eta^2 - F_{\eta\tau} = A(\tau), \tag{5.41}$$

where $\eta = z/h_0$, $\tau = Ut/h_0$, $R = Uh_0/\nu$,

$$\frac{p-p_0}{\rho} = \frac{1}{2}\frac{U^2r^2}{h_0^2}A(\tau) - 2U^2\left(\frac{1}{R}\frac{\partial F}{\partial \eta} + F^2 + \int_\eta^1 \frac{\partial F}{\partial \tau}\,\mathrm{d}\eta\right), \tag{5.42}$$

where A and the time-dependent reference pressure p_0 are unknown *a priori*. The boundary conditions for equation (5.41) require

$$F = F_\eta = 0 \quad \text{on} \quad \eta = 0; \tag{5.43}$$

$$F_\eta = 0, \quad F = -\frac{1}{2}\frac{\mathrm{d}\bar{h}}{\mathrm{d}\tau}, \quad \text{on} \quad \eta = \bar{h} = h/h_0; \tag{5.44}$$

$$F = 0 \quad \text{and} \quad \bar{h} = 1 \quad \text{at} \quad \tau = 0. \tag{5.45}$$

Two cases of special interest are: (i) when the fluid motion is induced by a constant downward force squeezing the fluid out radially and (ii) when the time-dependent gap width is prescribed. We consider each case in turn.

5.4.1 Constant force

The draining of fluid from the gap between the disks has been considered by Weinbaum, Lawrence and Kuang (1985) and Lawrence, Kuang and Weinbaum (1985) when a constant force is applied to the upper disk. Such a force may simply be the weight W of the upper disk, if it is assumed finite with radius a. In that case $h_0 \ll a$ must be assumed, and the solution (5.40), (5.42) will be appropriate everywhere except within a distance $O(h_0)$ from the edge. If the assumption is made that $h_{tt} \ll g$ then the force balance at the upper disk

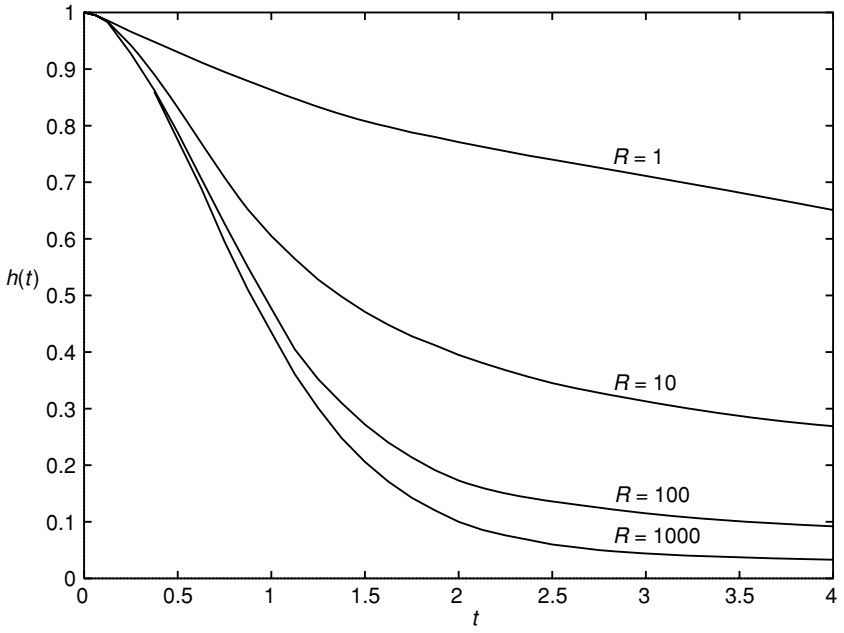

Figure 5.12 The gap width $h(t)$ for various values of the Reynolds number R.

requires $F_p = W$ where F_p is the force due to pressure at $z = h$ which, from (5.42), (5.44) is

$$F_p = \int_0^a 2\pi r p(r, h, t)\, \mathrm{d}r = \frac{\pi}{4}\rho U^2 \frac{a^4}{h_0^2} A + \rho\pi a^2 \left\{ p_0 - \frac{1}{2}U^2 \left(\frac{\mathrm{d}\bar{h}}{\mathrm{d}\tau} \right)^2 \right\}, \tag{5.46}$$

since $p(r, h, t) = \rho \left\{ U^2 r^2 A/2h_0^2 - U^2 \bar{h}_\tau^2/2 + p_0/\rho \right\}$. If the small drop in pressure across the exit is ignored, an approximation accurate to $O(h_0/a)$, and p is measured from the ambient pressure then $p_0/\rho = U^2\bar{h}_\tau^2/2 - U^2 a^2 A/2h_0^2$ and equation (5.46) then yields

$$F_p = -\frac{\pi\rho U^2 a^4 A}{4h_0^2} = W. \tag{5.47}$$

Weinbaum *et al.* have identified a characteristic settling velocity as $2(h_0/a) \times (W/\pi\rho a^2)^{1/2}$ and adopting this as the typical velocity U gives, from (5.47), $A(\tau) \equiv -1$. With this value for A, Lawrence *et al.* have integrated equation (5.41) numerically, subject to the conditions (5.43) to (5.45). Principal amongst the results is the variation of $\bar{h}$ with τ for different values of the Reynolds number R. These are shown in figure 5.12. Predictably the gap closes more

rapidly as the Reynolds number increases; for the high Reynolds number limit Lawrence *et al.* show that all the fluid is drained away when $\tau \approx 4$.

5.4.2 Prescribed gap width

Wang (1976) has extended his two-dimensional theory, discussed in section 4.8.2, to this axisymmetric situation. The two disks move relative to one another with the distance between them given as $h(t) = \pm h_0(1 - kt)^{1/2}$, so that initially they are separated by a distance $2h_0$. In this case, with an assumed symmetry of the flow about the mid-plane between the disks, it is convenient to take that plane as the origin for the co-ordinate z. With kh_0 as a characteristic velocity and

$$F(z,t) = \frac{f(\eta)}{4(1-kt)^{1/2}} \quad \text{where} \quad \eta = \frac{z}{h_0(1-kt)^{1/2}},$$

equation (5.40) gives

$$v_r = \frac{kr}{4(1-kt)} f'(\eta), \quad v_z = -\frac{h_0 k}{2(1-kt)^{1/2}} f(\eta), \tag{5.48}$$

so that, with $A = -A_0/8(1-kt)^2$, equation (5.41) gives as the ordinary differential equation for f,

$$\frac{2}{R} f''' + ff'' - \frac{1}{2} f'^2 - 2f' - \eta f'' = -A_0, \tag{5.49}$$

and the pressure is determined from (5.42) as

$$\frac{p - p_0}{\rho} = -\frac{k^2 r^2}{16(1-kt)^2} A_0 - \frac{h_0^2 k^2}{8(1-kt)} \left(4\frac{f'(\eta)}{R} + f^2(\eta) - 2\eta f(\eta) \right). \tag{5.50}$$

The boundary conditions for equation (5.49) require $f(0) = f''(0) = 0$ from the assumed symmetry about $z = 0$, and $f(1) = 1$, $f'(1) = 0$. That four conditions are required for the third-order equation (5.49) reflects the fact that $A_0 = -2f'''(1)/R$ is not determined *a priori*. In (5.50) the arbitrary time-dependent pressure $p_0(t)$ may be determined if, for example, the disks are assumed to be finite with radius $a \gg h_0$ and the pressure is equated with the ambient pressure, incurring an error $O(h_0/a)$. In particular if $p(a, h, t) = 0$ then

$$p_0(t) = \frac{\rho k^2 a^2}{16(1-kt)^2} \left\{ A_0 - 2\left(\frac{h_0}{k}\right)^2 (1-kt) \right\},$$

and

$$p(r,h,t) = \frac{\rho k^2 (r^2 - a^2) f'''(1)}{16R(1-kt)^2}. \tag{5.51}$$

Wang has obtained solutions of equation (5.49) for a range of values of R, both positive and negative. Qualitatively the results are similar to the two-dimensional case shown in figures 4.14 and 4.15, and not reproduced here. For $R > 0$, that is $k > 0$, $f'(\eta) > 0$ and fluid is squeezed radially outwards with increasing speed until the disks touch at $t = k^{-1}$. For negative k, and hence negative R, the disks are drawn apart. When $|R|$ is sufficiently small there is a unidirectional radial inflow between the disks with $f''(1) < 0$. However, when $R = R_{c_1} \approx -6.5$, $f''(1) = 0$, and for $R < R_{c_1}$ regions of radial outflow develop in the neigbourhood of each disk with a local maximum that increases with $|R|$ as in the two-dimensional case.

For a finite disk of radius a the pressure force F_p on the upper disk $\eta = 1$ is given, using (5.51), as

$$F_p = \int_0^a 2\pi r p(r, h, t)\, \mathrm{d}r = -\frac{\pi \rho k^2 a^4 f'''(1)}{32R(1-kt)^2}. \tag{5.52}$$

For $R > 0$ Wang finds that $f'''(1) < 0$, so that there is a net thrust on the two disks resisting their inward motion. For $R < 0$ Wang notes that for $R > R_{c_2} \approx -1.74$, $f'''(1) < 0$ but that for $R < R_{c_2}$, $f'''(1) > 0$. This implies that as the disks move apart there is a suction on them again resisting the motion for $R > R_{c_2}$, but for $R < R_{c_2}$ the force F_p in (5.52) is positive implying an outward thrust on the disks. However, care must be exercised in interpreting these results since for radial inflow, as when $R < 0$, the assumed self-similar form of solution cannot hold everywhere for a finite disk since no conditions at $r = a$ are imposed on the solution, and its range of validity is unknown.

The squeeze flows discussed above are axisymmetric. Wang and Watson (1979) consider squeeze flows in which this axisymmetry of flow properties is abandoned. With the gap width again prescribed as $h(t) = \pm h_0(1-kt)^{1/2}$ and the similarity variable $\eta = z/h_0(1-kt)^{1/2}$, the velocity components are written in a rectangular co-ordinate system as

$$\begin{aligned} u &= \frac{kx}{4(1-kt)} f_1'(\eta), \quad v = \frac{ky}{4(1-kt)} f_2'(\eta), \\ w &= -\frac{kh_0}{4(1-kt)^{1/2}} \{f_1(\eta) + f_2(\eta)\}, \end{aligned} \tag{5.53}$$

for which the corresponding pressure distribution may be written as

$$\begin{aligned} \frac{p}{\rho} = &-\frac{k^2 A_0 (x^2 + \alpha^2 y^2 - a^2)}{16(1-kt)^2} \\ &- \frac{k^2 h_0^2}{8(1-kt)} \left\{ \frac{2}{R}(f_1' + f_2') + \frac{1}{4}(f_1 + f_2)^2 - \eta(f_1 + f_2) \right\}. \end{aligned} \tag{5.54}$$

Table 5.1. *The two values of A_0, A_{01} and A_{02}, obtained when $R = -1$ for various values of α*

α	A_{01}	A_{02}
0.0	1.78647	−5.19816
0.2	1.75267	−7.72627
0.5	1.62476	−15.9346
0.7	1.50184	−27.0332
1.0	1.30226	−53.9867

The pressure $p(x, y, z, t)$ in equation (5.54) has been written in such a manner that for $a \gg h_0$, $p = 0$ at $x^2 + \alpha^2 y^2 = a^2$. An interpretation of this is that the planes which form the gap from which fluid is being squeezed are the ellipses $x^2 + \alpha^2 y^2 = a^2$, with semi-major and semi-minor axes a, b and $\alpha = a/b$. The equations satisfied by $f_i(\eta)$, $i = 1, 2$ are, from (1.9) and (1.10),

$$\frac{2}{R} f_i''' + \frac{1}{2}(f_1 + f_2) f_i'' - \frac{1}{2} f_i^2 - 2 f_i - \eta f_i'' = -A_0,$$

for which

$$f_i(0) = f_i''(0) = 0, \quad f_1(1) + f_2(1) = 2, \quad f_i'(1) = 0.$$

When $\alpha = 0$, $f_2 \equiv 0$ and the two-dimensional case is recovered, whilst for $\alpha = 1$, $f_1 \equiv f_2$ corresponding to the above axisymmetric case. Wang and Watson discuss briefly numerical solutions of the equations for $f_i(\eta)$ for a range of values of R and α with $0 \leq \alpha \leq 1$. In particular they conclude that for $R > 0$, that is when fluid is squeezed out between the plates, the solution is unique. However for $R < 0$, corresponding to separation of the plates, dual solutions have been discovered for all values of α in the range [0, 1]. Table 5.1 shows values of A_0 for various values of α when $R = -1.0$.

5.5 Rotating-disk flows

5.5.1 Self-similar flows

Self-similar time-dependent solutions, analogous to those considered in the previous section, have been considered by several authors. For example Watson and Wang (1979) consider an infinite disk rotating with angular velocity

$$\Omega(t) = \frac{\Omega_0}{1 - kt}. \tag{5.55}$$

Then, with velocity components

$$v_r = \frac{\Omega_0 r}{1-kt} f'(\eta), \quad v_\theta = \frac{\Omega_0 r}{1-kt} g(\eta), \quad v_z = -\frac{2(\nu\Omega_0)^{1/2}}{(1-kt)^{1/2}} f(\eta), \quad (5.56)$$

where $\eta = (\Omega_0/\nu)^{1/2} z/(1-kt)^{1/2}$, the continuity equation (1.22) is satisfied identically and, with the pressure given from equation (1.21) as

$$\frac{p-p_0}{\rho} = \frac{\nu\Omega_0}{1-kt}\{S\eta f(\eta) - 2f^2(\eta) - 2f'(\eta)\}, \quad S = \frac{k}{\Omega_0},$$

equations (1.19), (1.20) yield the following ordinary differential equations for $f(\eta)$, $g(\eta)$

$$f''' + 2ff'' - f'^2 + g^2 - S\left(f' + \tfrac{1}{2}\eta f''\right) = 0, \quad (5.57)$$

$$g'' + 2fg' - 2f'g - S\left(g + \tfrac{1}{2}\eta g'\right) = 0, \quad (5.58)$$

together with

$$f(0) = f'(0) = 0, \qquad g(0) = 1, \quad (5.59)$$

and

$$f'(\infty) = g(\infty) = 0. \quad (5.60)$$

Watson and Wang present solutions for a range of values of $S \leq 0$, indicating that no solutions exist for $S > 0$. The velocities therefore decay as t increases. The solutions have the properties that $g'(0) = 0$ for $S = S^* = -1.606699$, and $g'(0) \gtrless 0$ for $S \lessgtr S^*$. As the rate of decay of the disk rotation increases, that is as $|S|$ increases, the fluid close to the disk rotates more rapidly than the disk itself. For the special case $S = S^*$, for which $g'(0) = 0$, the torque on the disk vanishes, a case which Watson and Wang interpret as a situation corresponding to the decay of rotation of a free, massless disk in an infinite fluid. In figure 5.13 radial and azimuthal velocity profiles are shown for various values of S.

In the above example the fluid above the rotating disk is unbounded. Wang, Watson and Alexander (1991) consider a time-dependent rotating disk on which there is a liquid film of thickness $h(t)$. The angular velocity of the disk is again given by (5.55) with the velocity components as in equation (5.56). There is no radial pressure gradient so that f and g again satisfy (5.57), (5.58) and (5.59), but the conditions at the free surface now require careful consideration. At the surface of the film $v_z = \mathrm{d}h/\mathrm{d}t$ which indicates that $h(t)$ must be proportional to $(1-kt)^{1/2}$. Writing

$$h(t) = \left(\frac{\nu}{\Omega_0}\right)^{1/2} (1-kt)^{1/2}\beta, \quad (5.61)$$

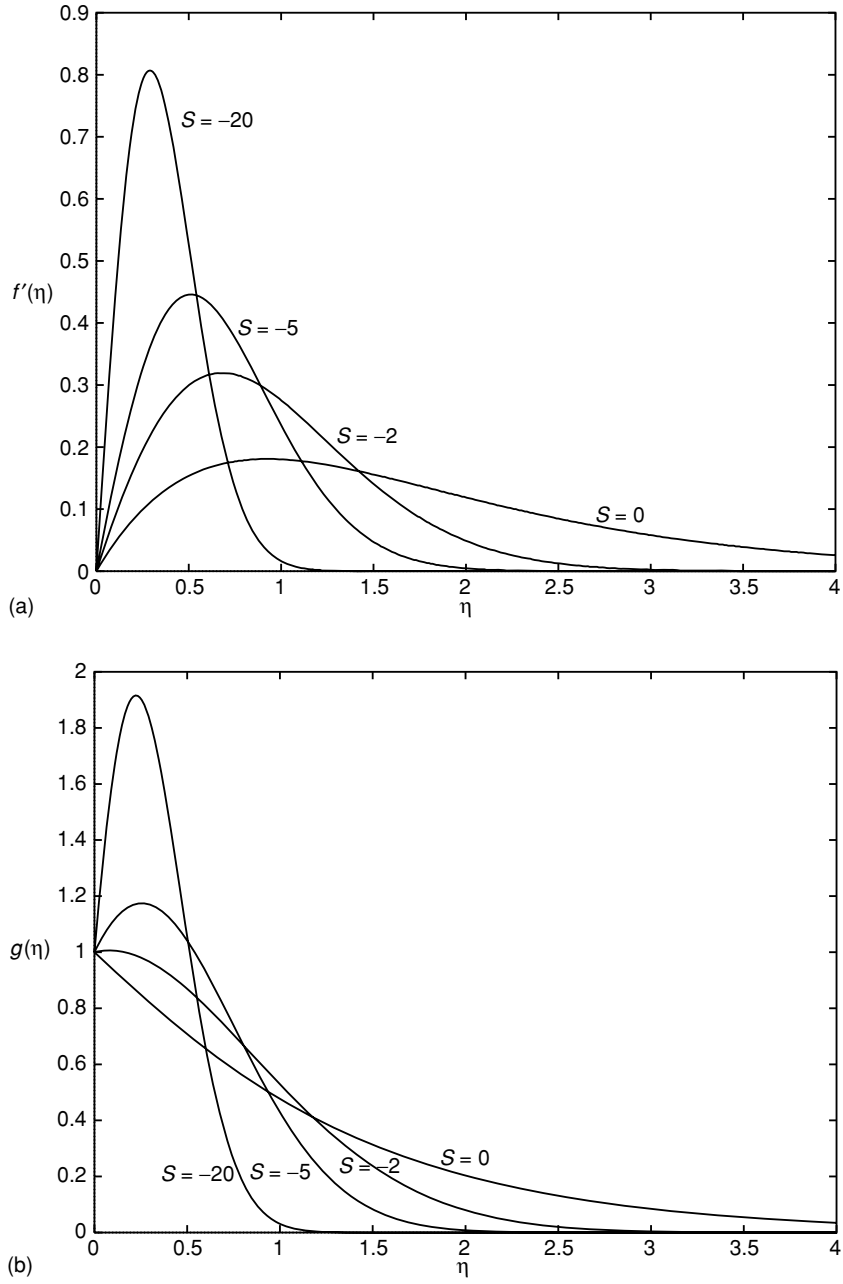

Figure 5.13 (a) The radial velocity profile $f'(\eta)$ for various values of S. (b) The azimuthal velocity profile $g(\eta)$ for various values of S.

the kinematic surface condition at $\eta = \beta$ is

$$f(\beta) = \frac{1}{4}\beta S \tag{5.62}$$

where, as before, $S = k/\Omega_0$. At the free surface the shear stress components vanish so that

$$f''(\beta) = g'(\beta) = 0. \tag{5.63}$$

As liquid is centrifuged radially outwards, the film thickness diminishes and, from (5.61), finally vanishes at $t = k^{-1}$. The unknowns $f(\eta)$, $g(\eta)$, β are determined from equations (5.57), (5.58) and the conditions (5.59), (5.62) and (5.63). Numerical solutions obtained by Wang *et al.* show that there are no solutions for $S > 0.588$ and that for $0 \leq S \leq 0.588$ two solutions exist. A summary of the dual solutions is shown in figure 5.14. For small values of β, f' is essentially parabolic with $g \approx 1$. But as β becomes large the liquid layer thickens, and indeed for S, $\beta^{-1} \to 0$ the solution approaches the steady von Kármán rotating disk solution, acknowledged by the intercepts for $f''(0)$, $g'(0)$ at $S = 0$ in figure 5.14(b). With p_0 the ambient pressure at $z = h$ the pressure in the liquid layer is given as

$$\frac{p - p_0}{\rho} = \frac{\nu\Omega}{1 - kt}\left\{S\eta f(\eta) - 2f^2(\eta) - 2f'(\eta) + 2f'(\beta) - \frac{1}{8}\beta^2 S^2\right\}.$$

Wang *et al.* have also discovered another branch of solutions for $-\infty < S < 0.0326$, but these have been rejected on physical grounds involving, as they do, negative radial velocity. Hamza and MacDonald (1984) also investigate the flow within a fluid layer of finite, but diminishing, thickness with an azimuthal velocity induced by not one, but two, rotating bounding surfaces. The flow may be interpreted as the squeeze flow of Wang (1976), discussed in section 5.4.2, upon which is superposed a rotation due to the rotation of one or both of the bounding disks. Adopting a notation in sympathy with the previously considered squeeze flows, the velocity components and pressure are written as

$$v_r = \frac{kr}{4(1 - kt)} f'(\eta), \quad v_\theta = \frac{\Omega_1 r}{(1 - kt)} g(\eta),$$

$$v_z = -\frac{kh_0}{2(1 - kt)^{1/2}} f(\eta), \quad \eta = \frac{z}{h_0(1 - kt)^{1/2}},$$

$$\frac{p - p_0}{\rho} = -\frac{A_0 k^2 r^2}{16(1 - kt)^2} - \frac{h_0^2 k^2}{8(1 - kt)}\left(\frac{4}{R} f'(\eta) - 2\eta f(\eta) + f^2(\eta)\right),$$

$$R = \frac{h_0^2 k}{\nu}.$$

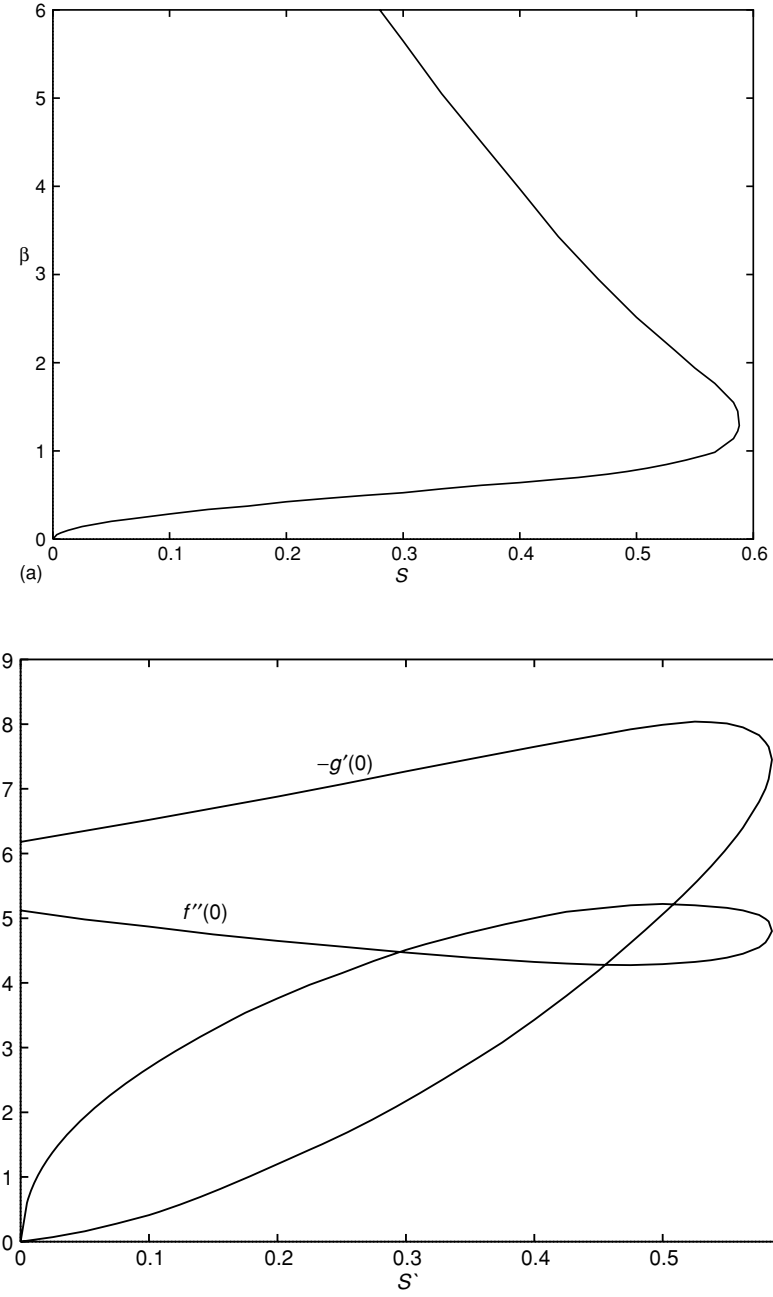

Figure 5.14 (a) Variation of the film thickness parameter β with S. (b) The radial and azimuthal shear-stress parameters $f''(0)$, $g'(0)$ as functions of S.

The continuity equation (1.22) is identically satisfied as is the normal momentum equation (1.21). The radial and azimuthal momentum equations will be satisfied provided that $f(\eta)$, $g(\eta)$ satisfy the ordinary differential equations

$$\frac{2}{R}f''' + ff'' - \frac{1}{2}f'^2 - 2f' - \eta f'' + \frac{8}{S^2}g^2 = -A_0, \tag{5.64}$$

$$\frac{2}{R}g'' + fg' - f'g - 2g - \eta g' = 0, \tag{5.65}$$

where $S = k\Omega_1$. The boundary conditions for equations (5.64), (5.65) will depend upon the relative rotation rates of the bounding disks. If one disk is at $z = 0$ rotating with angular velocity Ω_1, the other at $z = h_0(1 - kt)^{1/2}$, or $\eta = 1$, rotating with angular velocity Ω_2, then

$$f(0) = f'(0) = 0, \quad g(0) = 1; \quad f(1) = 1, \quad f'(1) = 0, \quad g(1) = \Omega_2/\Omega_1 = s. \tag{5.66}$$

The solution of (5.64) to (5.66) depends upon the three dimensionless parameters R, S and s; solutions are presented by Hamza and MacDonald for various values of these. The cases $s = 0$ and $s = -1$ are of particular interest. In the former case $f' > 0$ so that there is radial outflow throughout the fluid layer. For fixed R, as S decreases f' assumes a boundary-layer character close to $\eta = 0$ with $f'_{\max}$ increasing. For the case of counter-rotating disks, $s = -1$, the flow character changes significantly for R fixed as S decreases. For sufficiently large S, $f' > 0$, and there is radial outflow throughout with symmetry about $\eta = \frac{1}{2}$. However, as S decreases, whilst fluid close to each rotating disk continues to be centrifuged radially outwards, eventually an *inward* radial flow develops in the central portion of the fluid layer, with symmetry again maintained about $\eta = \frac{1}{2}$.

5.5.2 Rotating disk in a counter-rotating fluid

In section 3.5 on steady rotating disk flows it was noted that if, in the notation of equation (3.43), $\lambda_1 = \lambda_2 = 0$, $\lambda_3 = -1$ then no solution of equations (3.41), (3.42) exists (McLeod (1971)). Bodonyi and Stewartson (1977) have pursued this case by considering an initial-value problem and integrating the governing equations forward in time. The investigation seeks the nature of the solution as time increases which cannot, of course, be a steady state. If the disk rotates with angular velocity Ω in its own plane then (3.39) is replaced by

$$v_r = r\Omega f_\eta(\eta, \tau), \quad v_\theta = r\Omega g(\eta, \tau), \quad v_z = -2(\nu\Omega)^{1/2} f(\eta, \tau), \tag{5.67}$$

where $\eta = (\Omega/\nu)^{1/2} z$, $\tau = \Omega t$; and with the pressure given as

$$\frac{p - p_0}{\rho} = \frac{1}{2}\Omega^2 r^2 + 2\nu\Omega \left(\int_0^\eta f_\tau \, \mathrm{d}\eta - f^2(\eta) - f'(\eta) \right),$$

the equations satisfied by $f(\eta, \tau)$, $g(\eta, \tau)$, namely the unsteady analogues of (3.41), (3.42), are

$$f_{\eta\tau} - f_{\eta\eta\eta} - 2ff_{\eta\eta} - f_\eta^2 - g^2 + 1 = 0, \tag{5.68}$$

$$g_\tau - g_{\eta\eta} - 2(fg_\eta - f_\eta g) = 0, \tag{5.69}$$

with

$$f(0, \tau) = f_\eta(0, \tau) = 0, \quad g(0, \tau) = 1; \qquad f_\eta(\infty, \tau) = 0, \quad g(\infty, \tau) = -1. \tag{5.70}$$

The conditions at infinity reflect the fact that far from the rotating disk the fluid is in solid-body rotation with angular velocity $-\Omega$. Bodonyi and Stewartson integrate equations (5.68), (5.69), together with conditions (5.70), forward in time starting from the initial state $f(\eta, 0) = f_\eta(\eta, 0) = 0$, $g(\eta, 0) = -1$ for all η. The solution for g quickly develops a non-monotonic state with values of $g > 1$ and $g < -1$. Moreover the maximum values of both f_η and $|g|$ develop explosively for values of $\tau > 2$, such that the integration could not be continued beyond $\tau = 2.25$. The nature of the singular 'blow-up' of the solution was inferred heuristically from the behaviour of $f(\infty, \tau)$. Figure 5.15 illustrates this and, in particular, indicates that as $\tau \to \tau_s$, $f(\infty, \tau) \sim C/(\tau_s - \tau)^2$ where C is a constant and the singular time $\tau_s \approx 2.365$. This behaviour provides a starting point for the asymptotic analysis carried out by Bodonyi and Stewartson who show that both the radial and azimuthal velocity components break down as $(\tau_s - \tau)^{-1}$, as the singular time is approached.

The solution (5.67) is of separable type. Grundy and McLaughlin (1999) have considered the behaviour of a separable three-dimensional solution of more general type. The flow takes place between the planes $z = \pm h_0$ and, in Cartesian co-ordinates, with

$$u = kxf_1(\eta, \tau), \quad v = kyf_2(\eta, \tau), \quad w = -kh_0 g(\eta, \tau) \text{ where } \tau = kt, \eta = z/h_0,$$

the Navier–Stokes equations require

$$f_{i\eta\tau} - \frac{1}{R} f_{i\eta\eta\eta} - gf_{i\eta\eta} + (2f_i - g_\eta) f_{i\eta} = 0, \quad R = \frac{kh_0^2}{\nu}, \quad i = 1, 2;$$
$$f_1 + f_2 + g_\eta = 0. \tag{5.71}$$

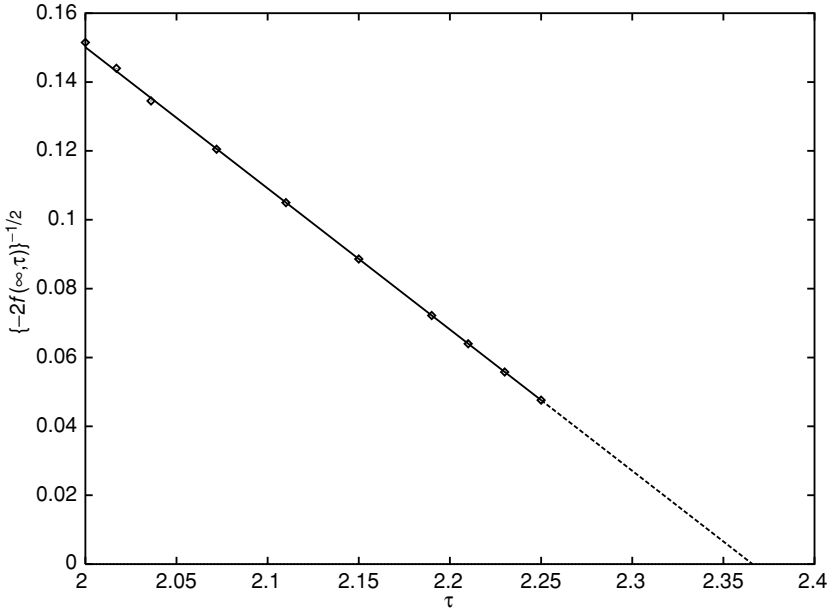

Figure 5.15 The linear variation of $\{-2f(\infty, \tau)\}^{-1/2}$ as $\tau \to \tau_s$ is demonstrated. The computed points are represented as $\diamond$, with the broken line a linear extrapolation to τ_s.

Although the problem as posed by Grundy and McLaughlin has its origin in solar magnetohydrodynamics, it does represent a type of stagnation-point flow. The plane $z = 0$ is assumed to be a plane of symmetry so that

$$f_{1\eta} = f_{2\eta} = g = 0 \quad \text{at} \quad \eta = 0, \tag{5.72}$$

and at $z = h_0$ the boundary is supposed porous with prescribed stresses so that

$$f_{1\eta} = \alpha, \quad f_{2\eta} = \beta, \quad g = \gamma \quad \text{at} \quad \eta = 1. \tag{5.73}$$

The system of equations (5.71) is seventh order and so an additional condition is required to supplement those set out in (5.72), (5.73). This is taken as $f_2(0, \tau) = \delta f_1(0, \tau)$ which, in some sense, characterises the geometry of the stagnation-point flow on $z = 0$. The equations (5.71) are integrated forward in time from initial distributions of f_1, f_2 and g of polynomial type that are consistent with (5.72) and (5.73). In some cases, for example when $R = 0.5$, $\alpha = \beta = -15$, $\gamma = 1, \delta = 0.5$, a steady state solution is attained; for others, for example when $R = 5$, $\alpha = \beta = -15$, $\gamma = 1$, $\delta = 0.5$ the solution blows up at a finite time. In those cases where the solution does terminate in a singularity, the singular

behaviour of u, v is as $(\tau_s - \tau)^{-1}$ and therefore similar to that exhibited in the problem addressed by Bodonyi and Stewartson (1977).

5.5.3 Non-axisymmetric flows

In section 3.5 attention has been drawn to the non-axisymmetric or eccentric flow between two parallel disks that rotate with the same angular velocity Ω but about different axes. Smith (1987) has included unsteady effects in such flows. In place of (3.51) the radial and azimuthal velocity components are written as

$$\begin{aligned} v_r &= \Omega l\{f(\eta,\tau)\cos\theta + g(\eta,\tau)\sin\theta\}, \\ v_\theta &= \Omega r + \Omega l\{g(\eta,\tau)\cos\theta - f(\eta,\tau)\sin\theta\}, \end{aligned} \tag{5.74}$$

with $v_z \equiv 0$ and the pressure given as

$$\frac{p - p_0}{\rho} = \frac{1}{2}\Omega^2 r^2 + \Omega^2 lr\{G(t)\cos\theta - F(t)\sin\theta\}. \tag{5.75}$$

The variables $\tau = \Omega t$, $\eta = z/h$ where h is the distance between the two disks; if only one disk is present then h is an arbitrary length. With the velocity components and pressure as in equations (5.74) and (5.75), equations (1.19) and (1.20) require

$$f_\tau - g - \frac{1}{R}f_{\eta\eta} = -G, \quad g_\tau + f - \frac{1}{R}g_{\eta\eta} = F, \quad \text{where again} \quad R = \frac{\Omega h^2}{\nu}. \tag{5.76}$$

The simplest situations arise when the upper disk is absent with fluid in the half-space $z \geq 0$ bounded by a single rotating disk at $z = 0$; for if the fluid at infinity rotates as a solid body with angular velocity Ω about the z-axis then $f, g \to 0$ as $\eta \to \infty$ and so $F = G \equiv 0$.

Consider first the case in which disk and fluid are in solid-body rotation about the common axis $r = 0$ for $\tau < 0$ and that the axis of rotation of the disk is moved impulsively from $r = 0$ to $r = l, \theta = \frac{1}{2}\pi$ at time $\tau = 0$. The boundary conditions for equations (5.76) are then

$$f = g = 0, \tau = 0, \eta > 0; f, g \to 0 \text{ as } \eta \to \infty; f = 1, g = 0, \eta = 0, \tau \geq 0. \tag{5.77}$$

Equations (5.76) subject to the conditions (5.77) may be solved using Laplace transform techniques. Thus the transforms $\bar{f}, \bar{g}$ of f, g are

$$\bar{f} = \frac{1}{2s}\left\{e^{-(s+i)^{1/2}\zeta} + e^{-(s-i)^{1/2}\zeta}\right\}, \quad \bar{g} = -\frac{i}{2s}\left\{e^{-(s+i)^{1/2}\zeta} - e^{-(s-i)^{1/2}\zeta}\right\},$$
$$\zeta = R^{1/2}\eta$$

which, upon inversion, give $f = \frac{1}{2}\mathrm{Re}(\phi)$, $g = \frac{1}{2}\mathrm{Im}(\phi)$ where

$$\phi = \mathrm{e}^{-(1+\mathrm{i})\zeta/\sqrt{2}}\,\mathrm{erfc}\left(\frac{\zeta}{2\sqrt{\tau}} - \frac{1+\mathrm{i}}{2\sqrt{2}}\sqrt{\tau}\right) + \mathrm{e}^{(1+\mathrm{i})\zeta/\sqrt{2}}\,\mathrm{erfc}\left(\frac{\zeta}{2\sqrt{\tau}} + \frac{1+\mathrm{i}}{2\sqrt{2}}\sqrt{\tau}\right).$$

As $\tau \to \infty$, $f \to \mathrm{e}^{-\zeta/\sqrt{2}}\cos(\zeta/\sqrt{2})$, $g \to -\mathrm{e}^{-\zeta/\sqrt{2}}\sin(\zeta/\sqrt{2})$ so that there is a final steady state in which

$$v_r = \Omega l\ \mathrm{e}^{-\zeta/\sqrt{2}}\cos(\theta + \zeta/\sqrt{2}), \quad v_\theta = \Omega r - \Omega l \mathrm{e}^{-\zeta/\sqrt{2}}\sin(\theta + \zeta/\sqrt{2}),$$

and each plane rotates with angular velocity Ω about an axis

$$r = l\exp\left\{-\left(\frac{R}{2}\right)^{1/2}\eta\right\}, \quad \theta = \frac{1}{2}\pi - \left(\frac{R}{2}\right)^{1/2}\eta.$$

In a further example the axis of rotation of the disk follows a circular orbit for $\tau > 0$ such that $f(0,\tau) = \cos\omega\tau$, $g(0,\tau) = -\sin\omega\tau$. The same technique may be used to determine f and g; in particular as $\tau \to \infty$ a periodic motion emerges with $f(\eta,\tau) = \mathrm{e}^{-\lambda\zeta}\cos(\omega\tau + \lambda\zeta)$, $g(\eta,\tau) = -\mathrm{e}^{-\lambda\zeta}\sin(\omega\tau + \lambda\zeta)$ where $\lambda = \{(1-\omega)/2\}^{1/2}$. A case of particular interest is when $\omega = 1$ so that the frequency of rotation of the fluid and that for the axis of the disk about the central axis are equal. For that case $f = \cos\tau\ \mathrm{erfc}(\zeta/2\sqrt{\tau})$, $g = -\sin\tau\ \mathrm{erfc}(\zeta/2\sqrt{\tau})$ and in the final state as $\tau \to \infty$

$$v_r = \Omega l\cos(\theta + \tau), \quad v_\theta = \Omega r - \Omega l\sin(\theta + \tau).$$

The velocity is independent of η; the rotation of the disk about its axis, and of its axis about the origin, combine to give eccentric solid-body rotation throughout the fluid. Smith observes that such a motion can always be induced by an appropriate periodic behaviour, period $2\pi/\Omega$, of the disk. This example in which the axis of rotation of the disk follows a periodic circular orbit has also been considered by Rao and Kasiviswanathan (1987).

The difficulties associated with the extension of the above to eccentric flow between two rotating disks have been discussed by Smith and are linked to the determination of $F(t)$, $G(t)$ in the expression (5.75) for the pressure. However, in the particularly important case

$$f(0,\tau) = -1, \quad g(0,\tau) = 0; \quad f(h,\tau) = 1, \quad g(h,\tau) = 0 \quad \text{for} \quad \tau \geq 0,$$

which yields the steady state solution of Abbott and Walters (1970) as $\tau \to \infty$, the mean position of the axis of rotation is $r = 0$ which is sufficient to ensure $F, G \equiv 0$. The solution may again be pursued by transform techniques, and

although the transform functions $\bar{f}(\eta, s)$, $\bar{g}(\eta, s)$ are not readily inverted they do yield the steady state solution of Abbott and Walters as $\tau \to \infty$.

In section 3.5.1 the work of Hewitt *et al.* (1999) was introduced in which asymmetry was introduced into the rotating-disk solution even though the boundary conditions favoured an axisymmetric solution. The same superposed asymmetry had earlier been introduced by Hall, Balakumar and Papageorgiu (1992). The solution proposed by Hall *et al.* may be written as

$$v_r = \Omega r\{f'(\eta, \tau) + \phi(\eta, \tau)\cos 2\theta\}, \quad v_\theta = \Omega r\{g(\eta, \tau) - \phi(\eta, \tau)\sin 2\theta\},$$
$$v_z = -2(\nu\Omega)^{1/2} f(\eta, \tau), \quad \text{where} \quad \tau = \Omega t \quad \text{and} \quad \eta = (\Omega/\nu)^{1/2} z,$$

with the pressure given by

$$\frac{p - p_0}{\rho} = \frac{1}{2}\lambda\Omega^2 r^2 + \nu\Omega P(\eta, \tau) + \Omega^2 r^2 Q(\tau)\cos 2\theta.$$

The continuity equation is satisfied identically and the momentum equations (1.19), (1.20), (1.21) give, for f, g, ϕ and P

$$f_{\eta\tau} - f_{\eta\eta\eta} - 2ff_{\eta\eta} + f_\eta^2 + \phi^2 - g^2 + \lambda = 0, \tag{5.78}$$
$$g_\tau - g_{\eta\eta} - 2fg_\eta + 2f_\eta g = 0, \tag{5.79}$$
$$\phi_\tau - \phi_{\eta\eta} - 2f\phi_\eta + 2f_\eta\phi + 2Q = 0, \tag{5.80}$$
$$P_\eta = 2f_\tau - 2f_{\eta\eta} - 4ff_\eta. \tag{5.81}$$

Whilst the main burden of their investigation centred upon unsteady motion, Hall *et al.* considered steady solutions of equations (5.78) to (5.80). The boundary conditions for these equations are

$$f = f_\eta = \phi = 0, \quad g = 1 \quad \text{at} \quad \eta = 0; \quad f_\eta, g \to 0, \quad \phi \to \gamma \quad \text{as} \quad \eta \to \infty \tag{5.82}$$

so that $\lambda = -\gamma^2$. The flow as $\eta \to \infty$ is, then, of a stagnation-point flow type. By contrast Hewitt *et al.* have $\gamma = 0$, but $g(\infty) = s \neq 0$ so that as $\eta \to \infty$ the flow is a solid-body rotation. In their numerical investigation of the resulting non-linear ordinary differential equations, Hall *et al.* reveal that for each value of γ there is a continuum of solutions arising from the decision to retain all solutions that decay exponentially and not rejecting those that decay most slowly. An illustration of the diverse solutions obtained is given in figure 5.16.

For unsteady flow attention is focused on the solution of (5.78) to (5.80) with γ and hence λ and Q equal to zero. The motivation is, in effect, to investigate the finite-amplitude instability of von Kármán's classical rotating-disk solution although, of course, the superposed finite-amplitude disturbances are restricted

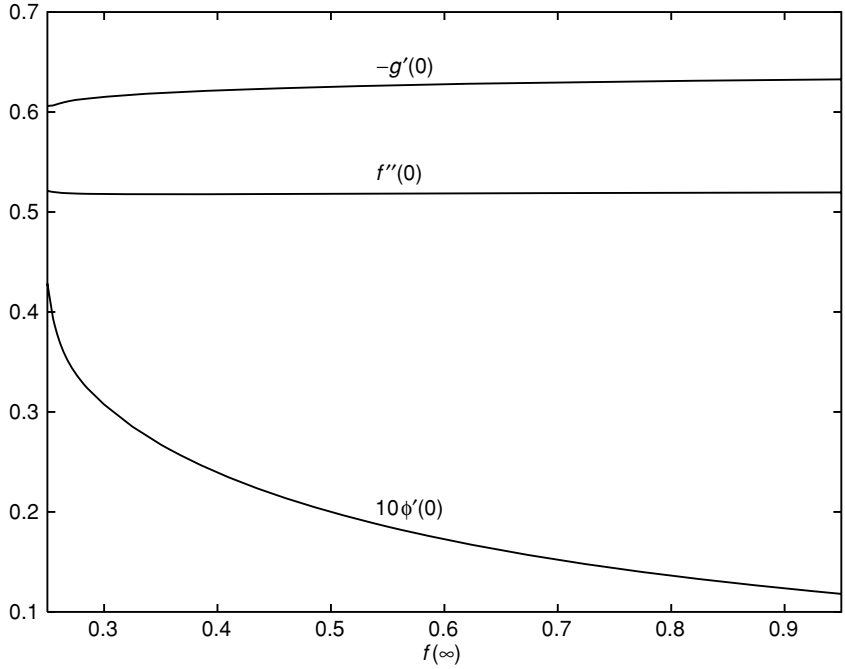

Figure 5.16 The shear-stress parameters $f''(0)$, $g'(0)$ and $\phi'(0)$ plotted as functions of $f(\infty)$.

to azimuthal wavenumber ± 2. The approach adopted is to integrate the equations forward in time. To enable this, initial conditions at $\tau = 0$ are required for f', g and ϕ; these are set as

$$f'(\eta, 0) = g(\eta, 0) = 0, \quad \phi(\eta, 0) = \delta\eta\, \mathrm{e}^{-(\eta-2)^2}, \tag{5.83}$$

and the calculations are carried out for values of $\delta = 0.35, 0.45, 0.55, 0.65$. For the two smaller values of δ the solution decays to the classical von Kármán solution. However, for the two larger values the solution terminates in a singularity at a finite time τ_s. In this 'blow-up' of the solution both v_r and v_θ exhibit behaviour $(\tau_s - \tau)^{-1}$ as $\tau \to \tau_s^-$, and so this is of the same type as observed in the blow-up of solutions encountered in the previous section.

5.5.4 An Ekman flow

In section 3.6 the classical steady Ekman (1905) solution is set out. In fact Ekman also considered an unsteady problem based on the impulsive start of

a uniform shear in the rotating system. Rott and Lewellen (1967) have also considered an oscillatory type of Ekman flow. If the boundary rotates with angular velocity Ω about an axis $\{x_c(t), y_c(t)\}$ then, in Cartesian co-ordidates, the velocity components at the plate are

$$u_w = -\Omega(y - y_c) + \frac{\mathrm{d}x_c}{\mathrm{d}t}, \quad v_w = \Omega(x - x_c) + \frac{\mathrm{d}y_c}{\mathrm{d}t},$$

and so, if

$$u = -\Omega y + Uh_1(z, t), \quad v = \Omega x + Uh_2(z, t)$$

then

$$U\{h_1(0, t) + \mathrm{i}h_2(0, t)\} = -\mathrm{i}\Omega\chi + \frac{\mathrm{d}\chi}{\mathrm{d}t} \quad \text{where} \quad \chi = x_c + \mathrm{i}y_c.$$

If a frame of reference rotating with angular velocity ω is introduced and $h(z, t)$ such that $h_1 + \mathrm{i}h_2 = h\mathrm{e}^{\mathrm{i}\omega t}$ then the real and imaginary parts of h are the Cartesian velocity components in this rotating frame. The equation satisfied by h is

$$\frac{\partial h}{\partial t} + \mathrm{i}(\Omega + \omega)h = \nu\frac{\partial^2 h}{\partial z^2}, \tag{5.84}$$

with

$$h(0, t) = \frac{1}{U}\left(-\mathrm{i}\Omega\chi + \frac{\mathrm{d}\chi}{\mathrm{d}t}\right)\mathrm{e}^{-\mathrm{i}\omega t}, \quad h \to 0 \quad \text{as} \quad z \to \infty.$$

If the centre of the boundary oscillates with frequency $\lambda/2\pi$ in this rotating frame then $\chi = l\,\mathrm{e}^{\mathrm{i}\omega t}\cos\lambda t$, and $h(0, t)$ becomes

$$h(0, t) = \frac{\mathrm{i}l}{2U}\{(\omega + \lambda - \Omega)\,\mathrm{e}^{\mathrm{i}\lambda t} + (\omega - \lambda - \Omega)\,\mathrm{e}^{-\mathrm{i}\lambda t}\}. \tag{5.85}$$

Defining quantities $\Lambda_\pm = \omega + \Omega \pm \lambda$, and assuming for simplicity that $\Lambda_\pm > 0$, the solution of (5.84) subject to (5.85) that decays as $z \to \infty$ is

$$h(z, t) = \frac{l}{U}(\omega + \lambda - \Omega)\,\mathrm{e}^{-(\Lambda_+/2\nu)^{1/2}z}\sin\left\{\left(\frac{\Lambda_+}{2\nu}\right)^{1/2}z - \lambda t\right\}$$
$$+ \frac{l}{2U}(\omega - \lambda - \Omega)\,\mathrm{e}^{-(\Lambda_-/2\nu)^{1/2}z}\sin\left\{\left(\frac{\Lambda_-}{2\nu}\right)^{1/2}z - \lambda t\right\}.$$

For $\Omega = 0$ Stokes' solution considered in section 4.1 is recovered, albeit with a rotating plane of oscillation.

5.6 Vortex motion

5.6.1 Single-cell vortices

In section 3.7.2 steady vortex flows in an unbounded fluid domain were considered of both single-cell (Burgers (1948)) and two-cell (Sullivan (1959)) structures. For a single-cell structure the radial velocity v_r does not change sign, whilst for a multi-cell structure v_r will change sign, once for the two-cell vortex of Sullivan.

For unsteady flow the classical solution of an isolated line vortex in an otherwise undisturbed fluid was first discussed by Oseen (1911) with

$$v_r = 0, \quad v_\theta = \frac{\Gamma}{2\pi r} g(r,t), \quad v_z = 0, \tag{5.86}$$

which may be compared with (3.63), (3.64). The equation for g is, from (1.20),

$$\frac{\partial g}{\partial t} = \nu \left(\frac{\partial^2 g}{\partial r^2} - \frac{1}{r}\frac{\partial g}{\partial r} \right),$$

and a solution which is regular at $r = 0$ and for which $g \to 1$ as $r \to \infty$ has

$$g(r,t) = 1 - \mathrm{e}^{-r^2/4\nu t}, \tag{5.87}$$

which may be compared with the solution (3.65). This solution (5.87) also has the property that $g \to 1$ as $t \to 0$ so that $v_\theta \sim \Gamma/2\pi r$, the potential vortex, in that limit. Initially, then, all the vorticity is concentrated along the axis $r = 0$. As t increases v_θ decreases at a given radial distance r, but as $r \to \infty$ the potential vortex solution is recovered with circulation Γ. The circulation about a closed circuit at large radial distances is, of course, unchanged since the total vorticity within it is unchanged. As $r \to 0$, at a fixed t, $v_\theta \sim \Gamma r/8\pi\nu t$, which shows that in the viscous core of the vortex the fluid is in solid-body rotation, with a diminishing angular velocity as t increases. In figure 5.17 the development of the flow is depicted.

Oseen's solution may be generalised by writing, instead of (5.86),

$$v_r = -\gamma(t) r, \quad v_\theta = \frac{\Gamma}{2\pi r} g(r,t), \quad v_z = 2\gamma(t) z \tag{5.88}$$

so that, from (1.20), g now satisfies

$$\frac{\partial g}{\partial t} - \gamma(t) r \frac{\partial g}{\partial r} = \nu \left(\frac{\partial^2 g}{\partial r^2} - \frac{1}{r}\frac{\partial g}{\partial r} \right). \tag{5.89}$$

This equation admits a self-similar solution with

$$\eta = \frac{r}{\phi(t)}, \tag{5.90}$$

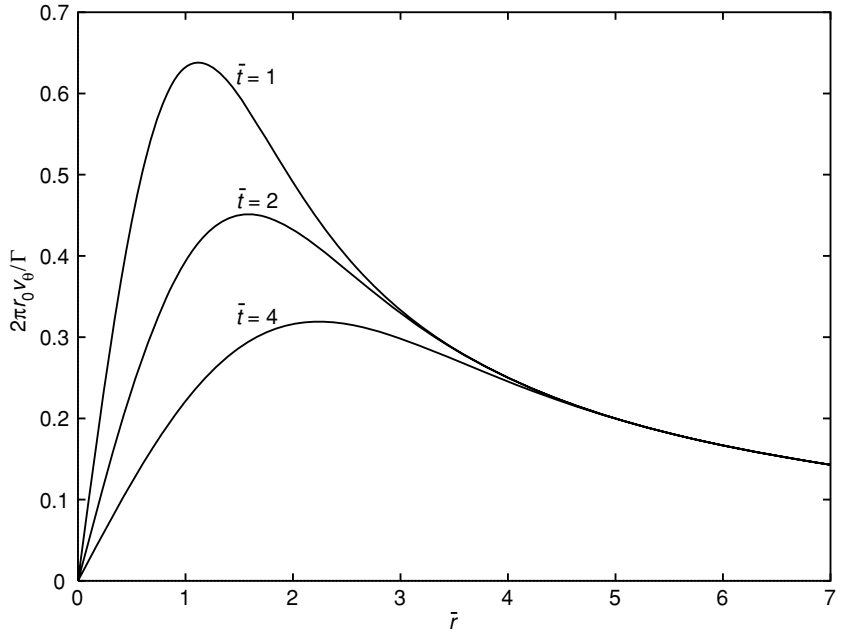

Figure 5.17 Velocity profiles in the classical Oseen (1911) vortex shown as a function of $\bar{r} = r/r_0$ for various values of $\bar{t} = 4\nu t/r_0^2$, where r_0 is an arbitrary length.

so that

$$-(\phi\dot{\phi} + \gamma\phi^2)\eta\frac{\partial g}{\partial \eta} = \nu\left(\frac{\partial^2 g}{\partial \eta^2} - \frac{1}{\eta}\frac{\partial g}{\partial \eta}\right) \tag{5.91}$$

provided that

$$\phi\dot{\phi} + \gamma\phi^2 = a, \quad \text{constant}, \tag{5.92}$$

in which case the solution for g is

$$g(r,t) = 1 - \mathrm{e}^{-a\eta^2/2\nu} = 1 - \mathrm{e}^{-ar^2/2\nu\phi^2}, \tag{5.93}$$

which may be compared with (5.87). Using (5.88) and (5.92) in equations (1.19) and (1.21) yields, for the pressure,

$$\frac{p - p_0}{\rho} = \frac{1}{2}\left\{(\dot{\gamma} - \gamma^2)r^2 - 2(\dot{\gamma} + 2\gamma^2)z^2 - \frac{\Gamma^2 a}{8\pi^2\nu\phi^2}\int_{ar^2/2\nu\phi^2}^{\infty}\left(\frac{1 - \mathrm{e}^{-s}}{s}\right)^2 \mathrm{d}s\right\}. \tag{5.94}$$

The solution is completed when ϕ is determined from (5.92). This first-order equation for ϕ^2 has solution

$$\phi^2 = 2a \exp\left(-2\int_0^t \gamma(s)\,\mathrm{d}s\right)\int_c^t \exp\left(2\int_0^u \gamma(s)\,\mathrm{d}s\right)\,\mathrm{d}u, \tag{5.95}$$

as in Rott (1958), where c is arbitrary.

Special cases of the unsteady stagnation-point flow represented by v_r and v_z in (5.88) may be considered. If $\gamma \equiv 0$ then $\phi = (2at)^{1/2}$ and Oseen's solution (5.87) is immediately recovered. The case $\gamma = k$, constant, has been discussed by Rott. This corresponds to the steady stagnation flow (3.63) and, indeed, if in (5.95) $c = -\infty$, $\phi^2 = a/k$ Burgers' solution (3.65) is recovered. For arbitrary c equation (5.95) yields

$$\phi^2 = \frac{a}{k}(1 + \beta\,\mathrm{e}^{-2kt}), \tag{5.96}$$

where β is arbitrary, so that the solution decays to Burgers' solution as $t \to \infty$. A case which exhibits singular behaviour at a finite time has been studied in detail by Moffatt (2000). With $\gamma = (t_s - t)^{-1}$ the corresponding solution of (5.95), with $c = -\infty$, is $\phi = \{2a(t_s - t)\}^{1/2}$. The flow develops from $v_\theta = 0$ at $t = -\infty$ to the potential vortex $v_\theta = \Gamma/2\pi r$ as $t \to t_s$, when the stagnation velocity components v_r, v_z become unbounded. Amongst the other possibilities, and they are endless, consider the following algebraically decaying stagnation flow for which $\gamma = 1/2(t_0 + t)$ so that, from (5.92), $\phi = a^{1/2}(t_0 + t)^{1/2}$ and hence

$$v_r = -\frac{r}{2(t_0 + t)}, \quad v_\theta = \frac{\Gamma}{2\pi r}\left(1 - \mathrm{e}^{-r^2/2\nu(t_0+t)}\right), \quad v_z = \frac{z}{(t_0 + t)}.$$

Then, as $t \to \infty$

$$v_r, \quad v_z \to 0, \qquad v_\theta \sim \frac{\Gamma}{2\pi r}\left(1 - \mathrm{e}^{-r^2/2\nu t}\right) = \frac{\Gamma}{2\pi r}\left(1 - \mathrm{e}^{-r^2/4\nu_e t}\right) \tag{5.97}$$

where $\nu_e = \nu/2$. The solution (5.97) incorporates the Oseen solution (5.87) but with an effective kinematic viscosity ν_e reflecting the different dynamical routes through which the flows have developed.

In the above examples the only component of the vorticity vector $\boldsymbol{\omega}$ is the axial component $\omega_z = (\Gamma/2\pi r)\,\partial g/\partial r$. An extension retains v_r, v_θ as in (5.88) but has $v_z = 2\gamma(t)z + W(r, t)$ so that there is, in addition to the axial component of vorticity, an azimuthal component $\omega_\theta = -\partial W/\partial r$. The equation (5.91) for $g(r, t)$ is unchanged with the choice (5.95) for $\phi(t)$, and with the pressure as in equation (5.94) the equation satisfied by $W(r, t)$ is, from (1.21),

$$\frac{\partial W}{\partial t} - \gamma r\frac{\partial W}{\partial r} + 2\gamma W = \nu\left(\frac{\partial^2 W}{\partial r^2} + \frac{1}{r}\frac{\partial W}{\partial r}\right). \tag{5.98}$$

Introducing the similarity variable (5.90) and employing the relationship (5.92) gives

$$\phi^2\left(\frac{\partial W}{\partial t}+2\gamma W\right)-a\eta\frac{\partial W}{\partial \eta}=\nu\left(\frac{\partial^2 W}{\partial \eta^2}+\frac{1}{\eta}\frac{\partial W}{\partial \eta}\right). \tag{5.99}$$

A separable solution of this equation with

$$W=f(t)\,\mathrm{e}^{-a\eta^2/2\nu}$$

gives, for $f(t)$,

$$\dot{f}+2\left(\gamma+\frac{a}{\phi^2}\right)f=0 \tag{5.100}$$

with formal solution

$$f(t)=C\exp\left[-2\int_0^t\left\{\gamma(s)+\frac{a}{\phi^2(s)}\right\}\,\mathrm{d}s\right].$$

The special case $\gamma(t)=k$, constant, for which ϕ is as in (5.96), has been considered by Gibbon, Fokas and Doering (1999) with the solution of (5.100) as

$$f=\frac{\mathrm{e}^{-4kt}}{\phi^2}=\frac{k}{a}(\mathrm{e}^{4kt}+\beta\,\mathrm{e}^{2kt})^{-1}.$$

So that for this special case $W(r,t)$ may be written as

$$W=(\mathrm{e}^{4kt}+\beta\,\mathrm{e}^{2kt})^{-1}\exp\{-kr^2(1+\beta\,\mathrm{e}^{-2kt})^{-1}/2\nu\}.$$

As $t\to\infty$, $W\to 0$, $\phi^2\to a/k$ and this solution again approaches the steady solution of Burgers as in equations (3.63) to (3.65).

5.6.2 Multi-cell vortices

Bellamy-Knights (1970) has introduced the analogue of the two-cell solution of Sullivan (1959), set out in equations (3.66), (3.67). In terms of the similarity variable $\eta=r/t^{1/2}$, Bellamy-Knights' solution may be written as

$$\begin{aligned} v_r&=\left(k-\frac{1}{2}\right)t^{-1/2}\left\{-\eta+\frac{6\nu}{k\eta}(1-\mathrm{e}^{-k\eta^2/2\nu})\right\},\\ v_\theta&=\frac{\Gamma}{2\pi r}\frac{g(\eta)}{g(\infty)},\qquad v_z=(2k-1)zt^{-1}(1-3\,\mathrm{e}^{-k\eta^2/2\nu}), \end{aligned} \tag{5.101}$$

where

$$g(\eta)=\int_0^{\eta^2/4\nu}\exp\left\{-u+3\left(1-\frac{1}{2k}\right)\int_0^u\left(\frac{1-\mathrm{e}^{-s}}{s}\right)\,\mathrm{d}s\right\}\,\mathrm{d}u,$$

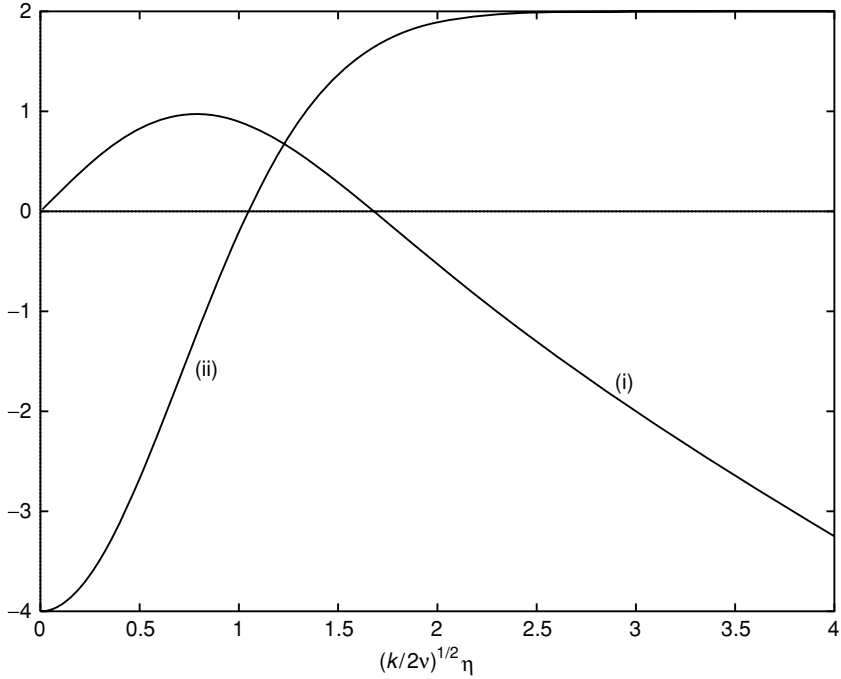

Figure 5.18 Velocity profiles in the two-cell vortex of Bellamy-Knights (1970). (i) $v_r(kt/2\nu)^{1/2}/(k-\frac{1}{2})$, (ii) $v_z(t/z)/(k-\frac{1}{2})$.

which may be compared with (3.66), (3.67). The corresponding expression for the pressure is

$$\frac{p-p_0}{\rho} = -\frac{(2k-1)}{8t^2}\{8(k-1)z^2+(2k+1)r^2\}$$
$$+\frac{9\nu^2(2k-1)^2}{2k^2}\frac{1}{t\eta^2}(1-\mathrm{e}^{-k\eta^2/2\nu})^2+\int_0^\eta \frac{v_\theta^2}{s}\mathrm{d}s.$$

Whilst only positive values of k are permitted if the solution is to remain bounded as $\eta\to\infty$, the character of the solution depends upon $k \gtrless \frac{1}{2}$ in the sense that there is radial inflow far from the axis if $k>\frac{1}{2}$, outflow if $k<\frac{1}{2}$. In figure 5.18 the radial and axial velocity components are shown. As k increases, the diameter of the inner cell, defined as the cylinder at which $v_r=0$, decreases due to the enhanced radial inflow. For all values of $k>\frac{1}{2}$ this bounding surface between the two cells contracts radially at a rate $\propto(\nu/t)^{1/2}$. Stream surfaces $z=z_0|-k\eta^2/2\nu+3(1-\mathrm{e}^{-k\eta^2/2\nu})|^{-1}$, where z_0 is an arbitrary constant, are shown in figure 5.19.

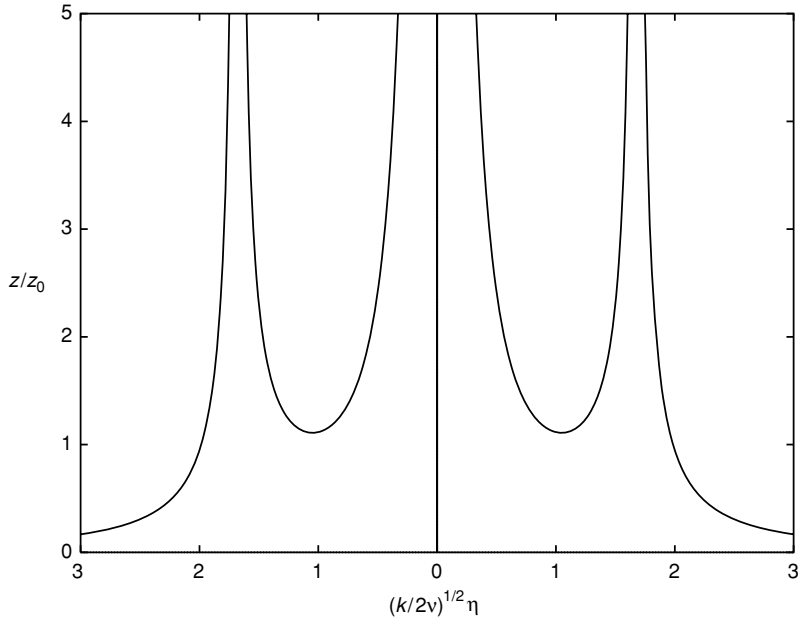

Figure 5.19 Stream surfaces of the two-cell vortex.

In a subsequent paper Bellamy-Knights (1971) has explored the possibility of extending the range of the multi-cell solutions set out in equation (5.101). Bellamy-Knights seeks solutions which have behaviour as $r \to \infty$ similar to that of the velocity components in equation (5.101) so that

$$v_r \sim -\frac{\gamma r}{2t}, \quad v_\theta \sim \frac{\Gamma}{2\pi r}, \quad v_z \sim \frac{\gamma z}{t} \quad \text{as} \quad r \to \infty. \tag{5.102}$$

A self-similar solution is available with

$$v_r = -\frac{2\nu}{r} f(\eta), \quad v_\theta = \frac{\Gamma}{2\pi r}\frac{g(\eta)}{g(\infty)}, \quad v_z = \frac{z}{t} f'(\eta) \quad \text{where now } \eta = \frac{r^2}{4\nu t}.$$

With the pressure given by

$$\frac{p - p_0}{\rho} = -\frac{1}{2}\gamma(\gamma - 1)\left(\frac{z}{t}\right)^2 - \frac{\nu}{t}\left(f(\eta) + f'(\eta) + \frac{f^2(\eta)}{2\eta}\right) + \frac{1}{2}\int_0^\eta \frac{v_\theta^2}{\eta}\,\mathrm{d}\eta,$$

equations (1.21) and (1.20) yield, respectively, equations for $f(\eta)$ and $g(\eta)$ as

$$(\eta f'' + \eta f')' + f f'' - f'^2 + \gamma(\gamma - 1) = 0, \tag{5.103}$$

and

$$\eta g'' + \eta g' + f g' = 0. \tag{5.104}$$

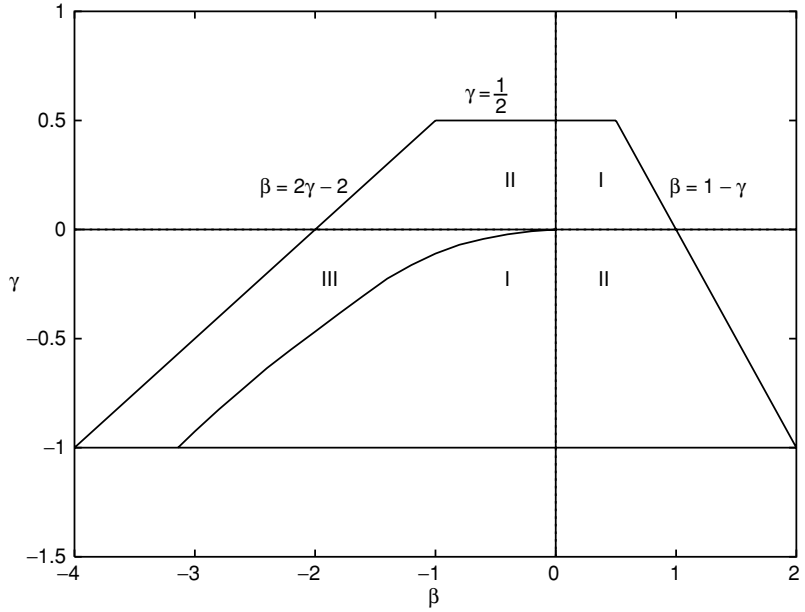

Figure 5.20 Regions of (β, γ)-space in which Bellamy-Knights (1971) finds: I, one-cell solutions; II, two-cell solutions; III, three-cell solutions.

The boundary conditions for equation (5.104) require $g(0) = 0$ if $v_\theta = 0$ at $r = 0$, and $g(\infty) = 1$ from (5.102). For equation (5.103), similarly, $f(0) = 0$ and $f'(\infty) = \gamma$. Bellamy-Knights also requires $f'''(0)$ to be finite at $\eta = 0$ so that $f''(0) = (\beta - \gamma)(\beta + \gamma - 1)$ where $f'(0) = \beta$ with the constant β unknown *a priori*. In the computational scheme the conditions adopted for (5.103) are

$$f(0) = 0, \quad f'(0) = \beta, \quad f''(0) = (\beta - \gamma)(\beta + \gamma - 1), \tag{5.105}$$

where a shooting method is adopted such that for each value of γ the value of β is chosen so that $f'(\infty) = \gamma$.

There are two exact solutions of (5.103), (5.104), (5.105). The first has $\gamma = \beta$ so that $f''(0) = 0$ and $f = \gamma\eta$ with $g = 1 - \exp\{-(1 + \gamma)\eta\}$. This is an example of the one-cell vortices in equation (5.88) with $v_r \propto r/t$. Another exact solution is available when $\gamma = -\beta/2$. In that case the solution of (5.103) is $f = \gamma\eta - \{3\gamma/(1 + \gamma)\}[1 - \exp\{-(1 + \gamma)\eta\}]$, which corresponds to the two-cell solution of equation (5.101) when $\gamma = 2k - 1$. A numerical investigation of (5.103), (5.105) has yielded further one- and two-cell solutions and, in addition, three-cell solutions. The regions of (β, γ)-parameter space in which these single- and multi-cell solutions have been found are shown in figure 5.20.

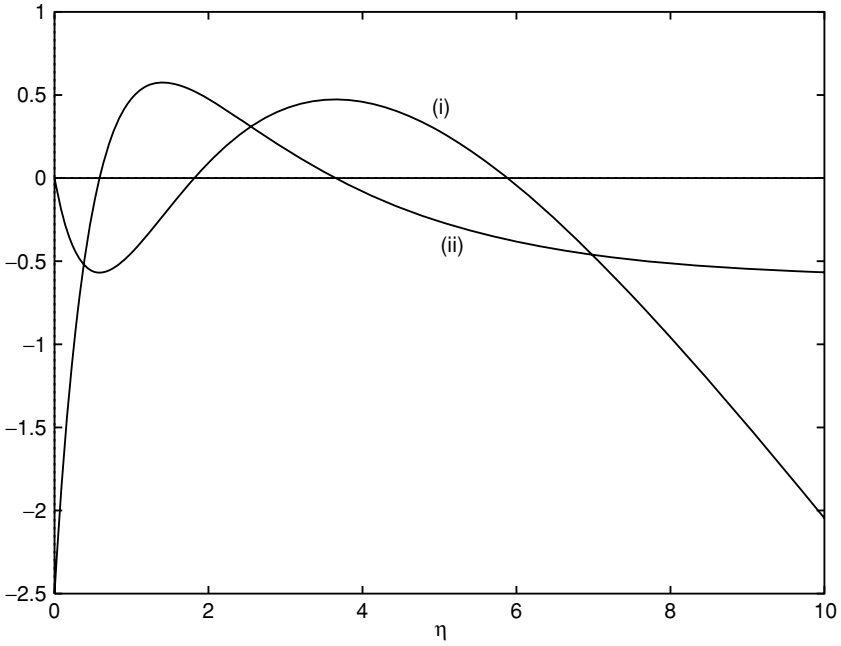

Figure 5.21 Velocity profiles for a three-cell vortex with $\beta = -2.5$, $\gamma = -0.6$. (i) $f(\eta) = -rv_r/2\nu$, (ii) $f'(\eta) = tv_z/z$, where $\eta = r^2/4\nu t$.

Apart from the analytic one- and two-cell solutions which are available for all $\gamma > -1$ on $\gamma = \beta$, $\gamma = -\beta/2$ respectively, other solutions have been found as follows (see figure 5.20). For $0 < \gamma < \frac{1}{2}$ solutions were obtained within the range $2\gamma - 2 < \beta < 1 - \gamma$; these are all of one-cell type for $\beta/\gamma > 0$ and two-cell type for $\beta/\gamma < 0$. For $-1 < \gamma < 0$ solutions were obtained for all β in the range $2\gamma - 2 < \beta < 1 - \gamma$; when $\beta > \beta_1(\gamma)$, where the boundary $\beta_1(\gamma)$ is determined numerically, the solutions are again one-cell for $\beta/\gamma > 0$ and two-cell for $\beta/\gamma < 0$. In the range $2\gamma - 2 < \beta < \beta_1(\gamma)$ three-cell solutions were found by Bellamy-Knights. These solutions, with $\gamma < 0$, all have the property that there is radial outflow from the vortex at large radial distances. By contrast it may be noted that Donaldson and Sullivan (1960) have established that only one- and two-cell solutions of the Burgers (1948) and Sullivan (1959) type exist for steady flow. In figure 5.21 radial and axial velocity profiles are shown for $\beta = -2.5$, $\gamma = -0.6$. The cylindrical cell boundaries are given by $v_r = 0$, and these increase again at a rate $\propto (\nu/t)^{1/2}$.The corresponding stream surfaces $z = z_0/|f(\eta)|$ are shown in figure 5.22.

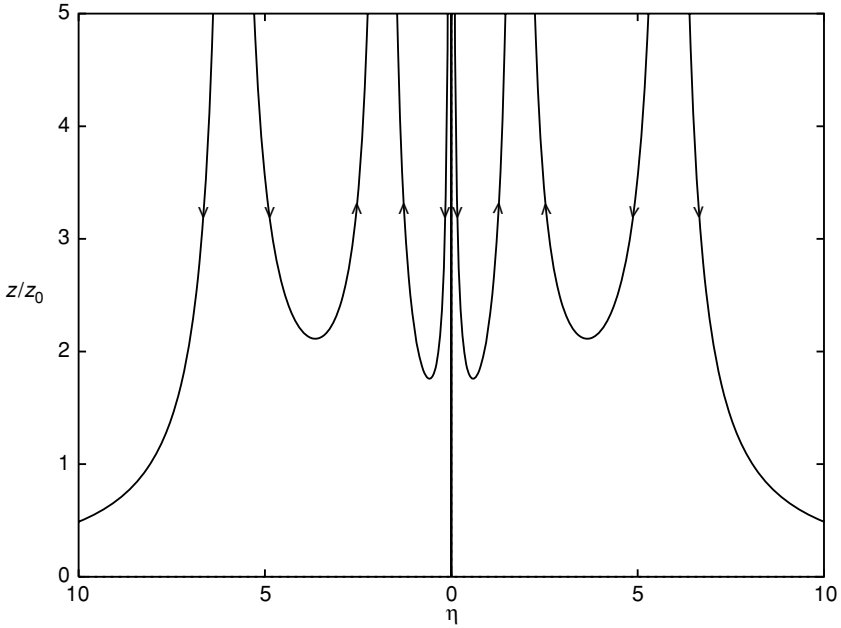

Figure 5.22 Stream surfaces corresponding to the profiles of figure 5.21.

For all of these multi-cell solutions $g(\eta) > 0$, increasing monotonically from zero to the unit asymptote so that the velocity distribution $v_\theta(r, t)$, at successive times, is qualitatively similar to the Oseen solution shown in figure 5.16.

5.6.3 The influence of boundaries

For the cellular vortex solutions, for example (5.88), (5.101), considered above all have the property that $v_z = 0$ at $z = 0$. The plane $z = 0$ may, then, be considered to be a solid boundary except, of course, the no-slip condition is not satisfied at it. One consequence, as in the steady-flow case, is that the strain rate and circulation at large distances are independent; see, for example, equation (5.101). Hatton (1975) introduces a no-slip boundary at $z = 0$, which couples the swirling and induced secondary motion, but finds that no exact solution is available corresponding to a potential vortex in the far field. Instead he proposes that at large distances from the boundary

$$v_r \sim -\frac{\gamma r}{2t}, \quad v_\theta \sim \frac{\Omega r}{4t}, \quad v_z \sim \frac{\gamma z}{t}, \tag{5.106}$$

which may be compared with (5.102). This corresponds to a flow established over the boundary which is in solid-body rotation with instantaneous angular velocity $\Omega/4t$ together with a radial and axial flow. Such solid-body rotation is a feature of the flow in the core of all the vortices considered above. Substituting (5.106) into equation (1.20) shows that it is necessary for $\gamma = -1$ so that in the core, away from the boundary, there is always a radial outflow and axial downflow.

With the velocity components and the pressure written as

$$v_r = \frac{r}{2t} f'(\eta), \quad v_\theta = \frac{\Omega r}{4t} g(\eta), \quad v_z = -2\left(\frac{\nu}{t}\right)^{1/2} f(\eta),$$

$$\frac{p - p_0}{\rho} = \frac{1}{32}(4 + \Omega^2)\left(\frac{r}{t}\right)^2 - \frac{2\nu}{t}\left\{f^2(\eta) + \frac{1}{2} f'(\eta) + \eta f(\eta)\right\},$$

where now $\eta = z/2(\nu t)^{1/2}$. Equations (1.19), (1.20) then give, as equations for f and g

$$f''' + 4ff'' - 2f'^2 + 4f' + 2\eta f'' + \tfrac{1}{2}\Omega^2 g^2 = \tfrac{1}{2}(4 + \Omega^2),$$
$$f(0) = f'(0) = 0, \quad f'(\infty) = 1,$$

and

$$g'' + 4(fg' - f'g) + 2\eta g' + 4g = 0,$$

with

$$g(0) = 0, \quad g(\infty) = 1.$$

The conditions at $\eta = \infty$ are determined by (5.106).

These equations for f and g have been integrated for a wide range of values of Ω. In all cases the behaviour of $g(\eta)$ is unexceptional with a monotonic increase to its asymptote. The behaviour of $f(\eta)$ is less straightforward. In figure 5.23 $f''(0)$ is shown as a function of Ω^2. For $\Omega^2 > 5$, $f''(0) < 0$ which means that there is a region close to the boundary, increasing with Ω^2, within which f, $f' < 0$ so that $v_r < 0$, $v_z > 0$, that is, radial inflow and axial upflow, before radial outflow and axial downflow are recovered in the far field. This implies the presence of a stagnation point on the axis. In figure 5.24 the location of this point is shown, together with the elevation at which v_r changes sign.

Hatton's work was motivated by the observed behaviour of tornadoes. There is visual evidence that close to the ground within the core of a vortex tornado there may be upflow or downflow with, in the former case, the upflow terminated by a stagnation point. The analysis of Hatton, based on the simple model that

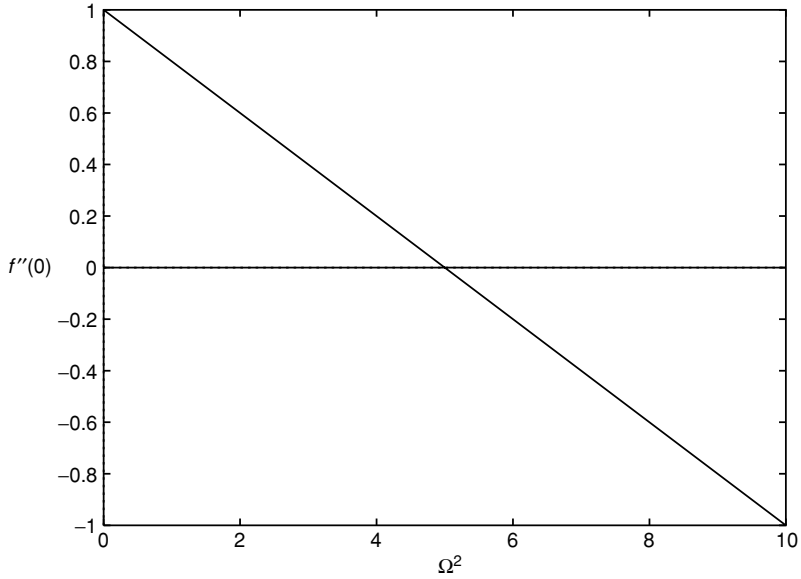

Figure 5.23 The shear-stress parameter $f''(0)$ as a function of Ω^2.

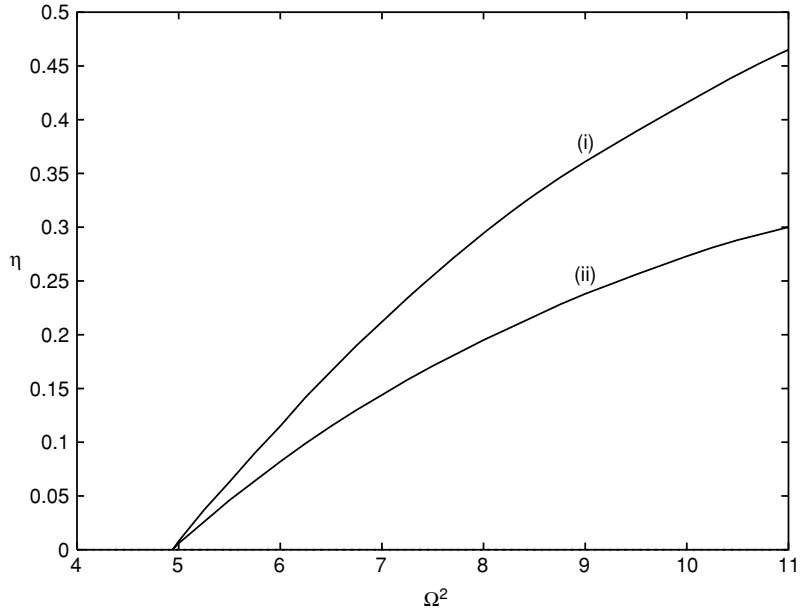

Figure 5.24 The variation with Ω^2 of: (i) the height of the stagnation point, (ii) the height at which the radial velocity component vanishes.

it is, suggests that either scenario is dynamically possible depending upon the angular velocity of the solid-body rotation within the core.

Öztekin, Seymour and Varley (2001) have discussed flows involving a vortex core together with a superposed flow sheared normal to the surface. For a class of unsteady flows both updraft and downdraft regions of flow are predicted.